Article

Ductile Versus Brittle Tectonics in the Anatolian–Aegean–Balkan System

Enzo Mantovani [1], Marcello Viti [1,*], Daniele Babbucci [1], Caterina Tamburelli [1], Massimo Baglione [2] and Vittorio D'Intinosante [2]

1   Dipartimento di Scienze Fisiche, Della Terra e dell'Ambiente, Università di Siena, 53100 Siena, Italy; enzo.mantovani@unisi.it (E.M.); babbucci@unisi.it (D.B.); tamburelli@unisi.it (C.T.)
2   Regione Toscana, Settore Prevenzione Sismica, 50129 Firenze, Italy; massimo.baglione@regione.toscana.it (M.B.); vittorio.dintinosante@regione.toscana.it (V.D.)
*   Correspondence: marcello.viti@unisi.it

Abstract: It is hypothesized that the present tectonic setting of the Anatolian, Aegean and Balkan regions has been deeply influenced by the different deformation styles of the inner and outer belts which constituted the Oligocene Tethyan system. Stressed by the Arabian indenter, this buoyant structure has undergone a westward escape and strong bending. The available evidence suggests that in the Plio–Pleistocene time frame, the inner metamorphic core mainly deformed without undergoing major fragmentations, whereas the orogenic belts which flanked that core (Pontides, Balkanides, Dinarides and Hellenides) behaved as mainly brittle structures, undergoing marked fractures and fragmentations. This view can plausibly explain the formation of the Eastern (Crete–Rhodes) and Western (Peloponnesus) Hellenic Arcs, the peculiar time-space features of the Cretan basins, the development of the Cyprus Arc, the North Aegean strike-slip fault system, the southward escapes of the Antalya and Peloponnesus wedges and the complex tectonic setting in the Balkan zone. These tectonic processes have mostly developed since the late Late Miocene, in response to the collision of the Tethyan belt with the Adriatic continental domain, which accelerated the southward bending of the Anatolian and Aegean sectors, at the expense of the Levantine and Ionian oceanic domains. The proposed interpretation may help us to understand the connection between the ongoing tectonic processes and the spatio-temporal distribution of major earthquakes, increasing the chances of estimating the long-term seismic hazard in the study area. In particular, it is suggested that seismic activity in the Serbo–Macedonian zone may be favored by the post-seismic relaxation that develops after seismic crises in the Epirus thrust front and inhibited/delayed by the activations of the North Anatolian fault system.

Keywords: Anatolian–Aegean–Balkan Tethyan belt; orogenic bending; ductile and brittle rheology

1. Introduction

The geodynamics of the complex tectonic evolution of the eastern Mediterranean region (Figure 1) is still subject to debate in the relevant literature. The aspect that stimulates most discussions is the development of extensional zones in a region stressed by the convergence of the confining plates (Nubia, Arabia and Eurasia). The most cited interpretation suggests that the Aegean extensional zone has been generated by the gravitational sinking of the Ionian slab (slab-pull mechanism, e.g., [1–7]). This hypothesis has been considerably encouraged by the velocity field delineated by geodetic observations (e.g., [8,9]), which shows a faster motion of the Aegean zone (30–40 mm/y) with respect to the Anatolian wedge (10–15 mm/y). However, this view does not consider that the present kinematics can be a transient phase of the post-seismic relaxation triggered by the strong seismic sequence that developed along the North Anatolian fault since 1939. The tentative simulation, by numerical modelling, of that perturbation [10,11] shows that the expected present velocity

field is very similar to the one defined by the geodetic data in the Anatolian–Aegean region. Furthermore, it must be pointed out that the almost uniform velocity field delineated by geodetic data in the Aegean area (e.g., [8,9]) is not compatible with the extensional regimes that generated the Cretan basins. The kinematic citations given in the text are always with reference to Eurasia.
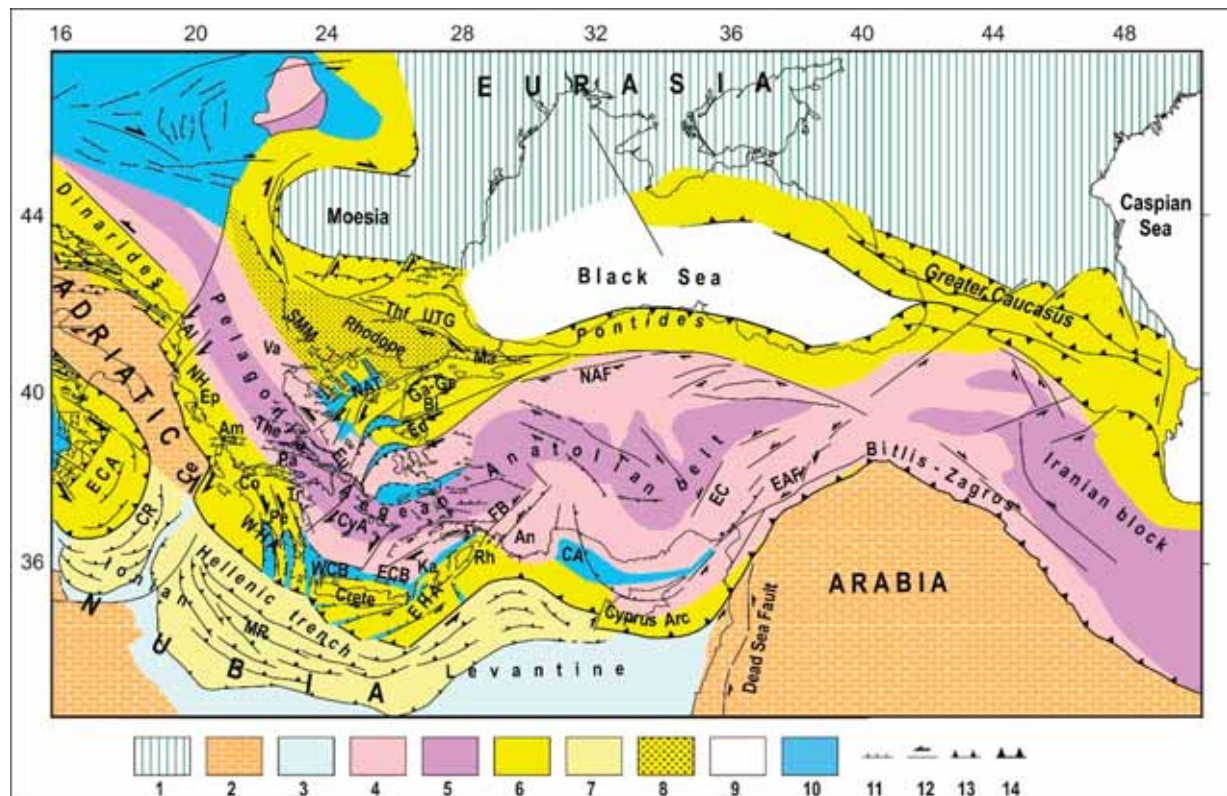

Figure 1. Tectonic scheme of the central and eastern Mediterranean area. (1) European continental domain, (2) Nubia–Adriatic continental domain, (3) Ionian–Levantine oceanic domain, (4, 5) inner belts of the Tethyan system, constituted by ophiolitic units and metamorphic massifs, respectively, (6) outer orogenic belts, (7) Calabrian and Mediterranean ridges, (8) Rhodope and Serbo–Macedonian (SMM) massifs, (9) Black Sea thinned domain, (10) Cenozoic basins, (11, 12, 13) extensional, transcurrent and compressional features, (14) outer fronts of the orogenic belts (references in the text). Al = Albanides, Am = Ambracique trough, An = Antalya peninsula, Bi = Biga peninsula, CA = Cilicia–Adana basin, Ce = Cephalonia fault, Co = Corinth trough, CR = Calabrian ridge, CyA = Cyclades Arc, EAF = Eastern Anatolian fault, EC = Ecemis faults, ECA = External Calabrian Arc, ECB = Eastern Cretan Basin, Ed = Edremit fault, EHA = Eastern Hellenic Arc, Eu = Eubea, FB = Fethiye–Burdur fault, Ga–Ge = Ganos–Gelibolu thrust fault, Ka = Karphatos, Ma = Marmara trough, MR = Mediterranean ridge, NAF = North Anatolian fault, NAT = North Aegean trough, NH = Northern Hellenides (Epirus), Pa = Parnassus, Pe = Peloponnesus wedge, Pl = Pliny fault, Rh = Rhodes, St = Strabo fault, The = Thessaly, Thf = Thrace fault, Tr = Trapezona, UTG = Upper Thrace graben, Va = Vardar zone, WCB = Western Cretan basin, WHA = Western Hellenic Arc.

Other authors [12–21], on the other hand, suggest that a dominant role in the evolution of the eastern Mediterranean region has been played by the westward extrusion of the Anatolian wedge and by the development of extrusion processes. This choice is supported by an accurate analysis of the compatibility of the proposed interpretation with the observed deformation pattern and of the major difficulties that the slab-pull model can encounter to explain such a pattern [17–23]. The main objectives of this work can be synthetized as follows. One aim is to provide further arguments in support of our previous interpretations of the study area, discussing in greater detail the compatibility between

the proposed driving forces and the observed deformation pattern in the Balkan zones. In particular, it is pointed out that the evolution of the Anatolian–Aegean system since the Late Miocene–Early Pliocene can be interpreted as the effect of two parallel belts that deform by different styles. The inner metamorphic chain behaves as a mainly ductile structure, undergoing only minor fragmentation, whereas the outer orogenic belts behave as mainly brittle structures, undergoing major fragmentations. This view is supported by the fact that seismicity is mainly related to the outer chains.

Another objective of this work is to provide a tentative explanation for the apparently ambiguous evidence on the strain regimes recognized in the Serbo–Macedonian zone on the basis of geological and geodetic data. Subsequently, some hypotheses are advanced about the possible relation between the proposed tectonic setting of the Anatolian and Aegean regions and the spatio-temporal distribution of major earthquakes since 1600. Some considerations are also devoted to the comparison of the expected effects of the major seismic sequence that developed along the North Anatolian fault since 1939 with the seismicity patterns in the Aegean and Balkan zones.

2. Geodynamics and Neogene Tectonic Evolution

The orogenic system that in the Oligocene separated the African and European domains (Iberian–Alpine and Tethyan belts, Figure 2a) was generated by the consumption of the Northern Neo Tethys domain since the Cretaceous and by the accretion of continental fragments interposed between small oceanic basins (e.g., [24–28]). The consumption and partial obduction of the oceanic domains generated ophiolitic belts (e.g., [29–32]), while underthrusting processes at continental collision boundaries generated the main metamorphic core [33–40]. As suggested by a number of authors (e.g., [26,34,41,42]), that orogenic system (Tethyan belt) was constituted by parallel chains: an inner core (Figure 2), consisting of oceanic remnants and crystalline massifs (Pelagonian–Cyclades–Anatolian), and two outer accretionary chains, one with European affinity (Carpathians, Balkanides and Pontides) and one with African affinity (Dinarides and Hellenides). The geometry of these belts shown in Figure 2 is only indicative.
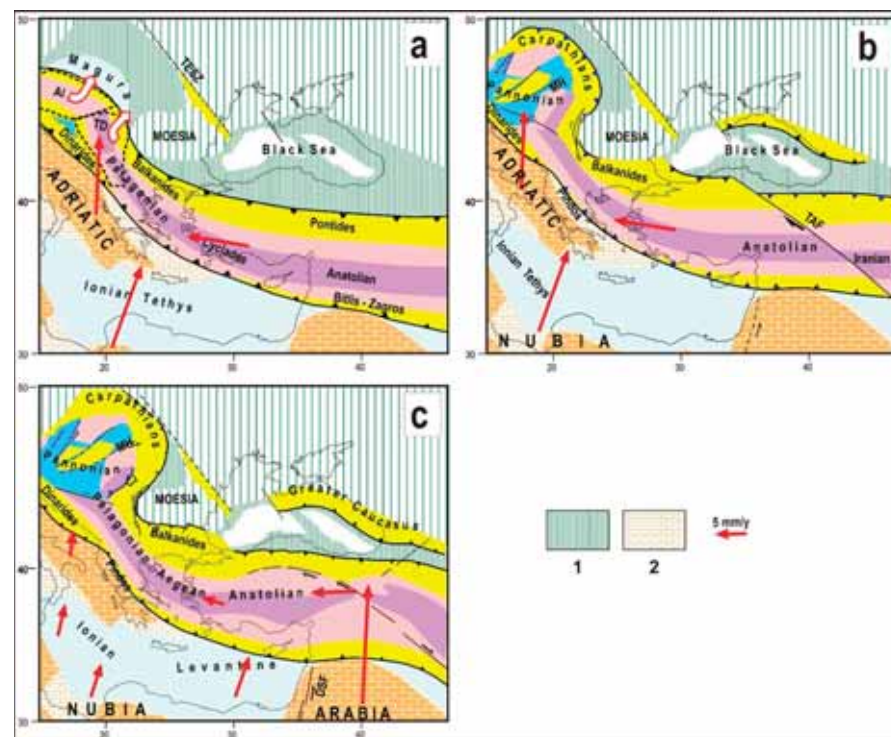

Figure 2. Proposed evolutionary reconstruction of the central–eastern Mediterranean region. (**a**) **Late Oligocene.** The Eurasian and African domains are separated by the Tethyan belt, formed by an inner

core (ophiolitic and metamorphic units, pink and violet, respectively), flanked by orogenic belts of European and African affinity (yellow). Al = Alcapa block, TD = Tisza-Dacia block, TESZ = Trans European Suture Zone (separating the European deformed sector from the East European Craton, [43]). (b) **Early Miocene.** Stressed by the Arabian indenter, the Tethyan belt migrates NW wards, at the expense of the oceanic and the thinned continental domains in the Magura zone. MH = Middle Hungarian fault, TAF = Trans Anatolian fault system. (c) **Middle-Late Miocene.** DSF = Dead Sea Fault. (1) Thinned continental Eurasian domain, (2) thinned continental Nubia/Adriatic domain. The kinematics with respect to a Eurasian reference frame [23,44] is tentatively indicated by the red arrows (scale in the inset). Present geographical contours (thin black lines) are reported for reference. Other colors and symbols as in Figure 1.

Stressed by the strong compressional context and uplift created by the Arabian indenter in the Late Oligocene, the Anatolian Tethyan belt decoupled from the European domain by a shear zone predating the NAF, i.e., the SE–NW Trans Anatolian decoupling fault system (e.g., [45–47]) and underwent a long NW-ward displacement (Figure 2b). This process may have been determined by the fact that in such structural/tectonic settings, the consumption of the oceanic and thinned continental domains in the Magura zone [48] was the most convenient shortening process. The migration path of that buoyant orogenic material was guided by the corridor that existed between the continental European domain (Moesia) and the continental Adriatic (e.g., [49]). The consumption of the Magura domain was produced by the opposite rotations of the Alkapa and Tisza blocks (Figure 2b). Back arc extension developed in the wake of these diverging blocks, forming the Pannonian basin. When the above trench zone sutured in response to the complete consumption of the thinned domains, around the Early–Middle Miocene ([50,51], Figure 2b), the deformation pattern of the Tethyan belt changed drastically, since the most convenient shortening process became the consumption of the Ionian and Levantine oceanic domains. This result was achieved by the SW-ward bendings of the Anatolian–Aegean Tethyan belt (Figure 2c, [19,20]).

This evolutionary phase lasted until the collision of the Aegean Tethyan belt with the continental Adriatic domain. Initially, this collision caused shortening and uplift in both the subsequent fold and thrust structures, occasionally affected by the inversion of previous normal faults in the Ionian domain during the Tortonian–late Messinian interval (e.g., [52]) and by thrusting and uplift in the western Aegean zone (Central Greece, [53,54]). Once the most thinned domains in the collision zone were consumed, the westward displacement of the extruding Anatolian wedge was accommodated by further bending of the Tethyan belt (Figure 3).

We advance the hypothesis that the very complex distribution of tectonic processes that developed during the Pliocene–Quaternary evolution in the study area (Figure 3b) was mainly conditioned by the different rheological behaviors of the inner Tethyan belt [55,56], which may have deformed as a mainly ductile medium, and the surrounding orogenic belts, which deformed undergoing major fragmentations, indicating a mainly brittle character. The ductile behavior can most reliably be inferred for the inner metamorphic belt (violet in Figure 1), while the pink belt, being only partially formed by metamorphic material (Ophiolites units), may deform with an intermediate style (between brittle and ductile). The computation of rheological profiles in the central and eastern Mediterranean area [55] indicates that the brittle upper crustal layer may reach 10 to 20 km, depending on the geothermal state. However, it is difficult to understand if this value may be taken as representative of the Plio–Quaternary situation.

The reliability of the above interpretation is checked by taking into account the strain regimes that the deformation of the inner core is expected to induce in the surrounding orogenic belts and analyzing their compatibility with the observed deformation patterns.
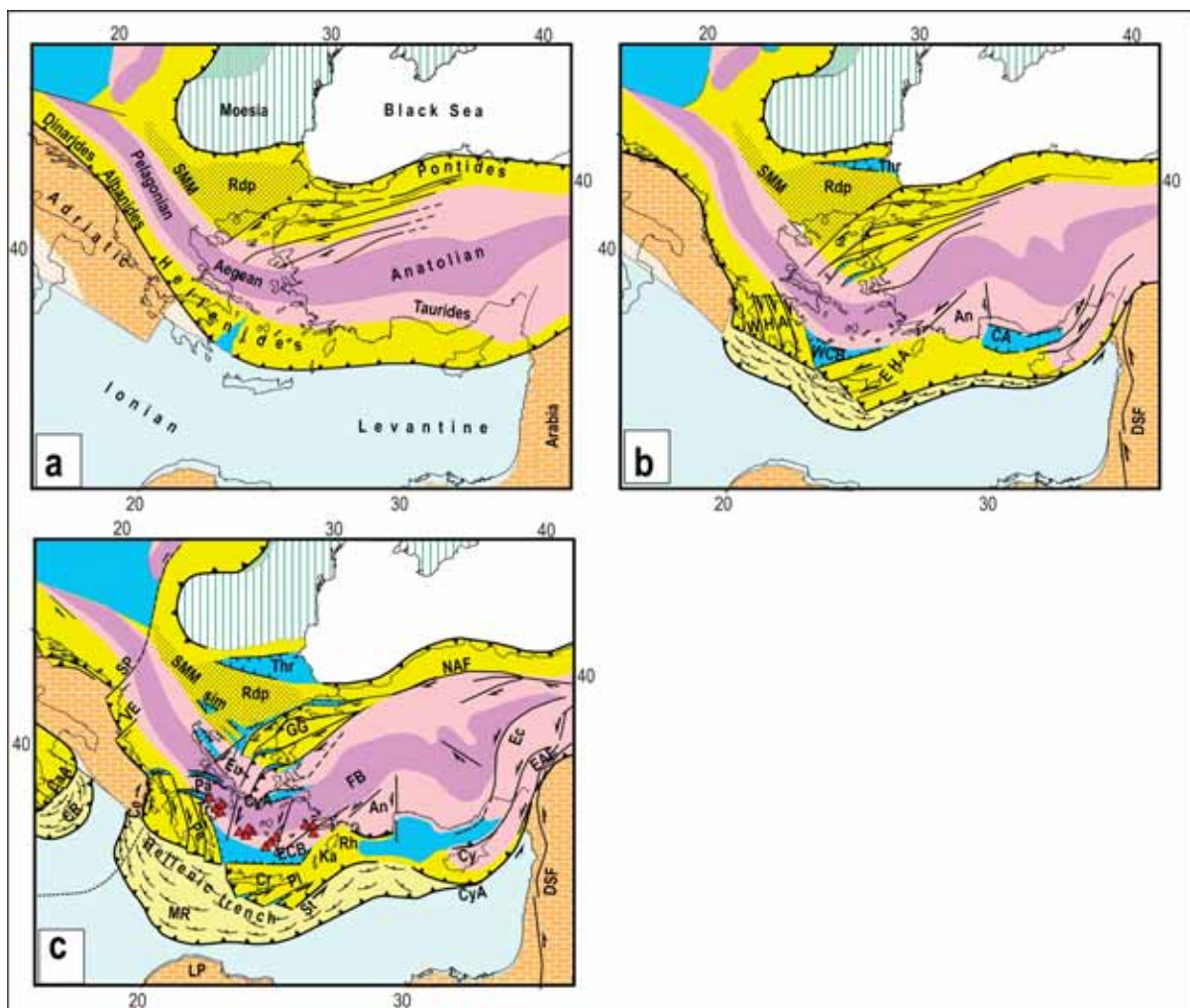
Figure 3. (**a**) **Late Miocene**. (**b**) **Upper Pliocene**. (**c**) **Pleistocene**. An = Antalia wedge, CaA = Calabrian Arc, Ce = Cephalonia thrust fault, Cr = Crete, Cy = Cyprus Arc, CyA = Cyclades arc, ECB = Eastern Cretan Basin, EHA = Eastern Hellenic Arc, Eu = Eubea, FB = Fethyie–Burdur fault, GG = Ganos–Gelibolu thrust zone, Ka = Karphatos, LP = Libyan promontory, Pa = Parnassus, Pe = Peloponnesus, Pl = Pliny fault, Rh = Rhodes, Rdp = Rhodope massif, Sim = Simitli graben, SMM = Serbo–Macedonian massif, St = Strabo fault, SP = Scutari–Pec fault, Thr = Thrace trough, Tr = Trapezona, VE = Vlora–Elbasan fault, WCB = Western Cretan basin, WHA = Western Hellenic Arc. The small red triangles along the southern border of the Cyclades massif indicate the calc-alkaline volcanic arc. Color, symbols and other abbreviations as in Figures 1 and 2.

A major example of the supposed ductile-brittle behavior may be recognized in the formation of the western (Peloponnesus) and eastern (Crete–Rhodes) Hellenic arcs (Figure 3a). Stressed by the convergence between the Anatolian block and the Adriatic plate, the inner belt (Cycladic arc) underwent southward bowing, without significant fragmentations, whereas the outer brittle belt, being affected by intense belt-parallel extensional stresses in its most curved zone, broke in two sectors, forming the western and eastern Hellenic arcs (Figure 3b). After separation, these two arcs progressively released their previous horizontal flexure, by clockwise (Peloponnesus) and counterclockwise (Crete–Rhodes) rotations. The consequent divergence between these belt sectors and the Cyclades massif (moderately deformed) induced the extension that formed the western Cretan basin, in the Early–Middle Pliocene (e.g., [57–59]). This interpretation can account for the almost triangular shape of that basin and for the timing of that event.

After its detachment from the eastern Hellenic Arc, the Peloponnesus wedge underwent E-W compression, driven by the convergence between the inner core (Cyclades massif) and Adria (Figure 3c, e.g., [60,61]). This shortening was accommodated by uplift and thrusting in the Epirus zone, while the compressional deformation pattern was more complex in the Peloponnesus wedge (Figure 3c). The difference was mainly caused by the SSW–NNE orientation of the southernmost Adria border, which created an asymmetric compressional mechanism. In such a context, the Aegean Tethyan belt underwent a clockwise bending (Figure 3c), which induced belt-parallel extensional stresses at its eastern side. This led to the formation of some E–W to SE–NW troughs, such as the Corinth and Ambracique, in the Peloponnesus sector, and the troughs that now separate the Trapezona, Parnassus and Eubea land structures, in the Greek inner belt (Figure 1). The effects of this mechanism were emphasized by the southward extrusion of the Peloponnesus slats [62,63]. The fact that the western guide of this extrusion (the Cephalonia fault) was shorter than the eastern one (inner Aegean Tethyan belt) produced an oblique escape, involving clockwise rotations of curved slats in the Peloponnesus (Figure 3c).

Another major example of ductile versus brittle tectonics is given by the development of the Cyprus arc [64–67]. The detachment of this belt sector from the main Anatolian body was caused by the strong bending it underwent at the outer side of the main central Anatolian curved sector, similarly to what happened in the Hellenic Arc. This detachment led to the formation of the Antalia and Cilicia–Adana basins (e.g., [68,69]).

The E–W to SSE–NNW convergence between the Anatolian wedge, on one side, and the Rhodope massif and the Adriatic continental domain, on the other side, (Figure 3b,c) induced E–W compression in the northwestern Anatolian corner and in the northern–central Aegean zone (e.g., [54,57,70–72]). Contemporaneously, these zones were stressed by N–S to NNW–SSE extension, induced by the southward bending of the inner Aegean core (Figure 3c). The combined effect of these deformations led to the formation of a system of dextral transtensional faults in the northern Aegean and northwestern Anatolian zones [3,73–76].

The present slab under the Aegean zone is identified by intermediate earthquakes, reaching a depth of about 130–140 km [77,78]. Another evidence about the oceanic subducted lithosphere under the Aegean area is given by the calc-alkaline and high-K calc-alkaline geochemical signature of the volcanic arc located along the southern margin of the Cyclades Arc (Figure 3c, [79]). A very interesting feature of this magmatic arc is the fact that its western and central—eastern sectors developed in rather different times. The western part (Aegina, Methana and the oldest volcanic rocks of Milos and Santorini) formed in the Early Pliocene, while the central and eastern sectors (Milos, Santorini, Nisyros, e.g., [78,80,81] and references therein) date back to the Middle–Late Pleistocene.

Since these times correspond well to the formations of the western Cretan basin (Early Pliocene) and the central–eastern Cretan basin (mid to late Quaternary), one may suppose that all magmas were generated at the same time (i.e., when the slab reached the opportune depth), but their uprise was only allowed by the formation of transtensional fault systems in the upper crust of the western and eastern Cretan basins. The possible connection between pull-apart transtensional features and volcanic activity is suggested by what happened in many other zones, such as the Roman and Campanian volcanism in the Italian region [82,83] and elsewhere (e.g., [74,84–90]).

The westward displacement of the central Anatolian body and the contemporaneous SE-ward bending of the western Anatolia metamorphic belt (Figure 3) induced E–W compression in the interposed zone. This mechanism may explain the SW-ward escape of the Antalya wedge, guided by the Fethiye–Burdur fault. Since at that time the Antalya zone was still connected with the eastern Hellenic arc, the above extrusion also involved the Crete–Rhodes sector, accelerating its SW-ward motion. Around the early Pleistocene, this mechanism led to the collision of the Crete–Rhodes sector with the Lybian promontory. Resisted by this obstacle, the southern part of Crete (Figure 3c) slowed down, whereas the main Crete slat was only deviated, assuming the present E–W orientation. The relative

motion between main Crete and the resisted southern slats was allowed by the formation of the Pliny and Strabo faults (Figure 3). The clockwise rotation and westward displacement of the Cretan slat can explain the formation of the eastern Cretan basin and the interruption of the land continuity with Karpathos and Rhodes [57,62,91].

Pushed by the Tethyan belt, the Northern Hellenides belt (Epirus) was forced to migrate westward, overthrusting the Adriatic domain (Figure 3). The decoupling of this belt sector from the southern Dinarides was accommodated by the formation of dextral shear faults, such as the Scutari–Pec and Vlore–Elbasan, and by the clockwise rotation of the Albanides [92,93].

The Neogene–Quaternary tectonic setting in the Balkan zone (Pelagonian, Vardar, Serbo–Macedonian and Rhodope structures) is mostly recognized as related to S–N to SW–NE extension (e.g., [3,94–99]), but the driving mechanism of this strain regime is still subject to debate. Some authors suggest a connection with the extensional process that formed the Aegean zone (e.g., [3]).

In our opinion, the Plio–Quaternary deformation pattern in the SMM zone can be explained as an effect of two driving mechanisms, both induced by the westward displacement and deformation of the Tethyan belt. One is the westward push of northern Anatolia on the Rhodope massif. The zone where this push is exerted corresponds to the Ganos–Gelibolu thrust zone, where Pliocene compressional deformations are recognized ([100], Figure 3). This interaction causes a roughly NW-ward displacement, along with a clockwise rotation, of the Rhodope massif (Figure 3). The consequent divergence between this massif and the European domain (Moesia) induced the dextral transtensional regime that formed the upper Thrace trough. (Figure 3, [3,19,101]). If this was the only driving mechanism, one could expect compressional deformation in the zone stressed by the Rhodope massif, i.e., the Serbo–Macedonian massif (SMM). To explain why this last zone is instead characterized by S–N extension, one must consider the effects of the other driving mechanism that induces E–W extension in the SMM, i.e., the roughly westward displacement of the Pelagonian–Vardar units, as a part of the Tethyan belt (Figure 3c). In fact, the relative motion between the Rhodope massif (moving roughly NW-ward) and the Pelagonian–Vardar belt (moving roughly west- to WNW-ward) induces a S–N extension in the interposed zone, i.e., the SSM.

Another obstacle against a full understanding of tectonics in this zone is given by the fact that geodetic observations in the Simitli graben (SMM) indicate compressional deformations and uplift (Pirin horst) [102], in contrast to the extensional regime indicated by geological evidence [3,94–99]. We suggest that this puzzling problem can find a plausible solution by supposing that the present shortening recognized in the Simitli graben is a transient phase of the stress field perturbation that was triggered by the strong earthquakes that occurred along the NAF from 1939 to 1999. Such a sequence allowed a remarkable westward displacement of northern Anatolia [103], increasing its push on the Rhodope massif and consequently compression in the SMM zone. Such processes, propagated with velocities controlled by post-seismic relaxation, are expected to reach the SMM zone after several decades from the triggering events [10,11]. Thus, it is reasonable to suppose that the compressional stress field involved by the above event is still affecting the SMM zone. This hypothesis is supported by the monitoring of the strain rate at some points in the Simitli graben in the time interval 1980–2010 (Struma and Krupnic faults, [102]), which show that the 1999 strong Izmit earthquake (M = 7.4), along the western NAF, determined a remarkable increase in shortening in the observation points.

Since it is widely recognized that an increase in compression on a fault zone tends to inhibit or at least delay the occurrence of major earthquakes, the present compressional stress field in the Simitli graben could indicate a low probability of major earthquakes in that zone. This possibility can find important support from the fact that since 1940 (during the NAF seismic sequence), only very few earthquakes (with M < 6) occurred in the SMM zone (Figure 4).
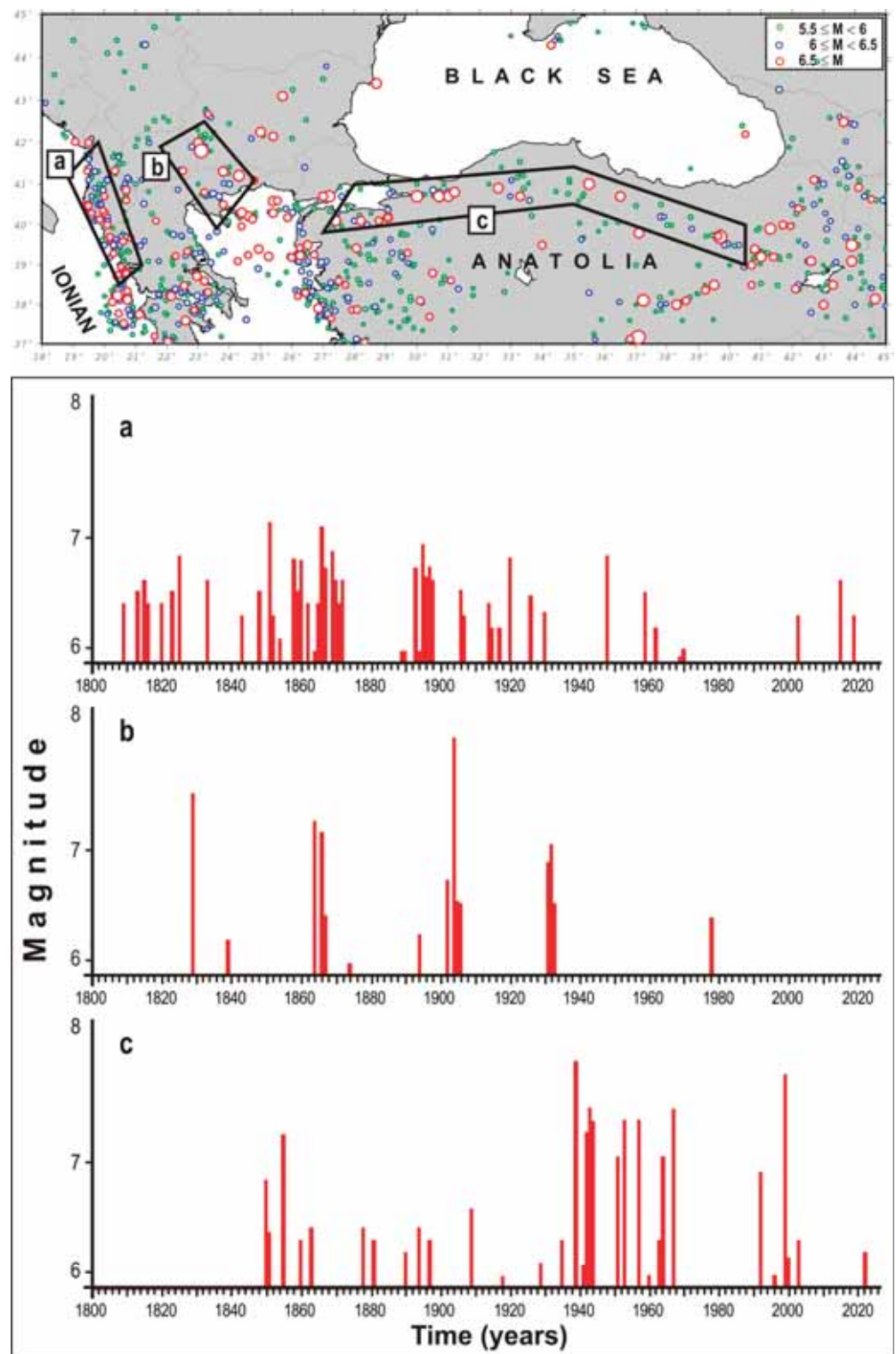
Figure 4. Time patterns of main earthquakes that occurred in the Epirus thrust zone (**a**), the Serbo–Macedonian massif (**b**) and NAF (**c**) zones since 1800. The geometries of the zones considered are shown on the map. Seismicity data by [104–116].

The distribution of major earthquakes shown in Figure 4 can also support another basic concept of seismotectonics, i.e., the hypothesis that an increase in extensional stresses on a fault is expected to favor seismic activity. The most convincing evidence in this regard is given by the fact that the strongest earthquakes in the SMM zone just occurred during or

after major seismic crises in the Epirus zone (Figure 4), which are supposed to induce E–W extension in the SMM zone [19].

3. Main Seismic Zones

The distribution of major earthquakes that occurred since 1600 (Figure 5a) can provide an idea about the location of the seismogenic faults in the study area. Focal mechanisms and geological data allow the recognition of the strain fields in the main seismic zones (Figure 5b).
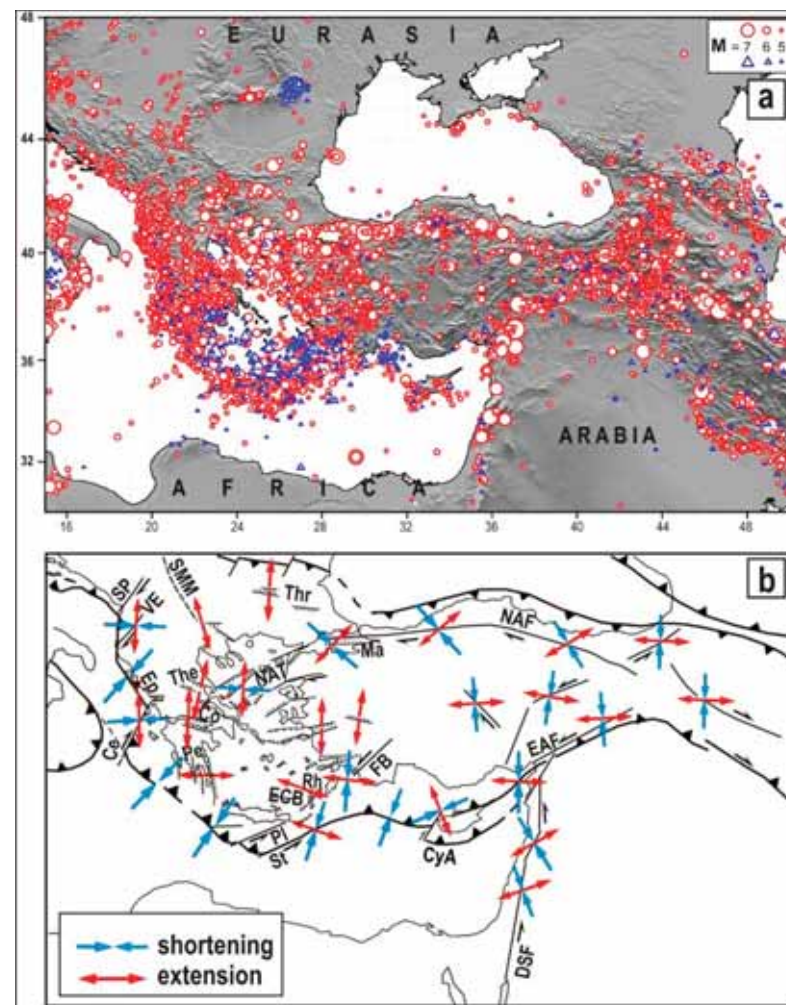

Figure 5. (**a**) Major earthquakes (M > 5) that occurred since 1600 A.D. Seismicity data as in Figure 4 and by [117–124]. (**b**) Strain fields in the main seismic zones inferred from focal mechanisms and geological data (See the references in the text). Abbreviations as in Figure 1.

In the Albania zone, seismicity is associated with SE–NW compression (Albanides thrust fronts), segmented by two main NE–SW dextral transversal faults, i.e., the Scutari–Pec and Vlora–Elbasan [92,125–128].

In the Epirus zone, NW–SE to S–N thrust faults dominate, allowing the belt units to overthrust the southern Adriatic domain (e.g., [129–131]).

In the Cephalonia fault zone, dextral transpressional focal mechanisms, associated with a significant uplift, are related to the overthrusting of the Peloponnesus wedge on the Adriatic plate (e.g., [132–134]). This fault system is interpreted as the surface expression of a tear fault which decouples the Hellenic slab from the Adriatic continental margin that underthrusts the Northern Hellenides (e.g., [135]).

The central part of Greece is undergoing a roughly S–N extensional regime, mainly evidenced by focal mechanisms in the Corinth, Ambracique and Thessaly grabens [60,81,136–138]. This regime is compatible with the southward extrusion of the Peloponnesus wedge, in response to E–W compression [19].

The Northern Aegean and Northwestern Anatolian regions are cut by a system of dextral NE–SW transtensional faults [139,140], with a progressive increase in the extensional component from east to west (e.g., [136]). In the northern Aegean, those faults bound morphological depressions, such as the Sporades, Skiros and Ikaria. The north Aegean fault system is connected with the North Anatolian fault through the Ganos transpressional lineament and the Marmara pull-apart trough [15,19,141–143]. The northwestern Anatolian zone is characterized by prominent E–W grabens (e.g., [144]). The stress field is dominated by N–S extension, compatible with the source of the recent 2020 Samos earthquake (M = 7.0, [145] and references therein).

In the SMM zone, most authors (e.g., [3,96–99,146,147]) suggest that the main faults were generated by N–S extension. In the upper Thrace graben, along the northern side of the Rhodope massif, N–S to NE–SW extension is recognized (e.g., [3,101]). The focal mechanism of the strong 1928 destructive earthquake (Plovdiv, Bulgaria, M = 6.8 and 7.1) indicates a WNW–ESE oriented normal fault with a significant dextral component [148].

In SW Anatolia, a NE–SW shear zone, known as Fethiye–Burdur fault (Figure 1) has been identified along the western side of the Antalya wedge (e.g., [149]). Strong earthquakes in the southernmost sector of this fault, near the Rhodes basin (e.g., 1957, M = 6.8, 7.2; 2012, M = 6.2), indicate NE-trending sinistral strike-slip mechanisms [150].

In the Eastern Hellenic arc, both GPS observation and earthquakes focal mechanisms suggest NE–SW sinistral transpressional deformation on the outer side (Pliny and Strabo trenches) and prevalent extensional regime on the internal side, with orientations of the extensional principal axis progressively varying from NW–SE in eastern Crete to E–W in the Cretan and Karpathos basins [81,151,152].

The North Anatolian fault (NAF) is mainly characterized by right-lateral strike-slip deformation. Slip rates based on GPS data (20–25 mm/y (e.g., [8]) are significantly greater than the rates inferred from geological evidence (6.5 mm/y in the eastern sector, to 17–19 mm/y in the western sector, e.g., [15,153]). The western NAF divides into two or three sub-parallel strands [15,154], where source mechanisms indicate transpressional (e.g., Ganos fault, [100,155]) or transtensional (e.g., Edremit gulf, [156,157]) regimes. It can be noted that earthquakes with M ≥ 7.5 only occurred in the eastern NAF [158].

The Eastern Anatolian fault (EAF) is dominated by left-lateral strike-slip motion along the main strand, which extends about 700 km in N60° E direction (e.g., [159]). Towards SW, it connects with the N35° E Amanos fault and then with the N–S Dead Sea fault. Sub-parallel branches split from EAF, giving rise to restraining and releasing (pull-apart) bends, with reverse and normal components in the relative strike slip solutions [160]. Two major earthquakes occurred in 2023 (M = 7.8, 7.7), one in the main strand, almost at the intersection with the Amanos fault, and the other in the northern, E–W oriented strand. Another strong event (M = 6.7) occurred in 2020, northeast of the above bifurcation [161]. Geological and geomorphological studies indicate EAF slip rates decreasing from the northeastern (10 mm/y), to the southwestern (4 mm/y) sectors, in agreement with geodetic data ([160] and references therein).

4. What Can We Learn from the Post-1939 Seismic Sequence Along the NAF?

This work suggests that the Neogene tectonic activity in the Aegean zone has been driven by the westward extrusion of the Anatolian wedge. To check if this context is still going on, it is useful to investigate the possible tectonic implications of the seismic sequence that activated the entire NAF since 1939. For instance, one can try to understand the possible connection between the time pattern of seismicity in the Aegean zone and the expected effects of the above seismic sequence (Figure 6a,b). To make this check, one must consider that the strain perturbation triggered by that sequence travelled with velocities

controlled by the rheological properties of the structures involved, as suggested by the concepts of post-seismic relaxation [162,163]. In this regard, we take into account the results obtained by [10,11], who tried to reproduce the effects of the post-seismic relaxation induced by a sudden westward displacement of Anatolia. The resulting time pattern of the induced strain energy rate in the central Aegean zone (Figure 6c) shows the highest values in the time interval 1950–1970. The fact that during the same phase the number of major earthquakes (M > 5.5) in that zone was higher than in the other time intervals (Figure 6b) suggests that seismotectonic activity in the Aegean area may be mainly conditioned by the westward accelerations of Anatolia. If the extensional seismotectonic activity was mainly driven by slab-pull forces, the effects of the post-1939 seismic sequence would have attenuated rather than increased seismic activity in the Aegean zone. This is because a SW-ward motion of the northern Aegean zone (induced by post-1939 relaxation) would have reduced the divergence of this zone from the retreating Hellenic arc.
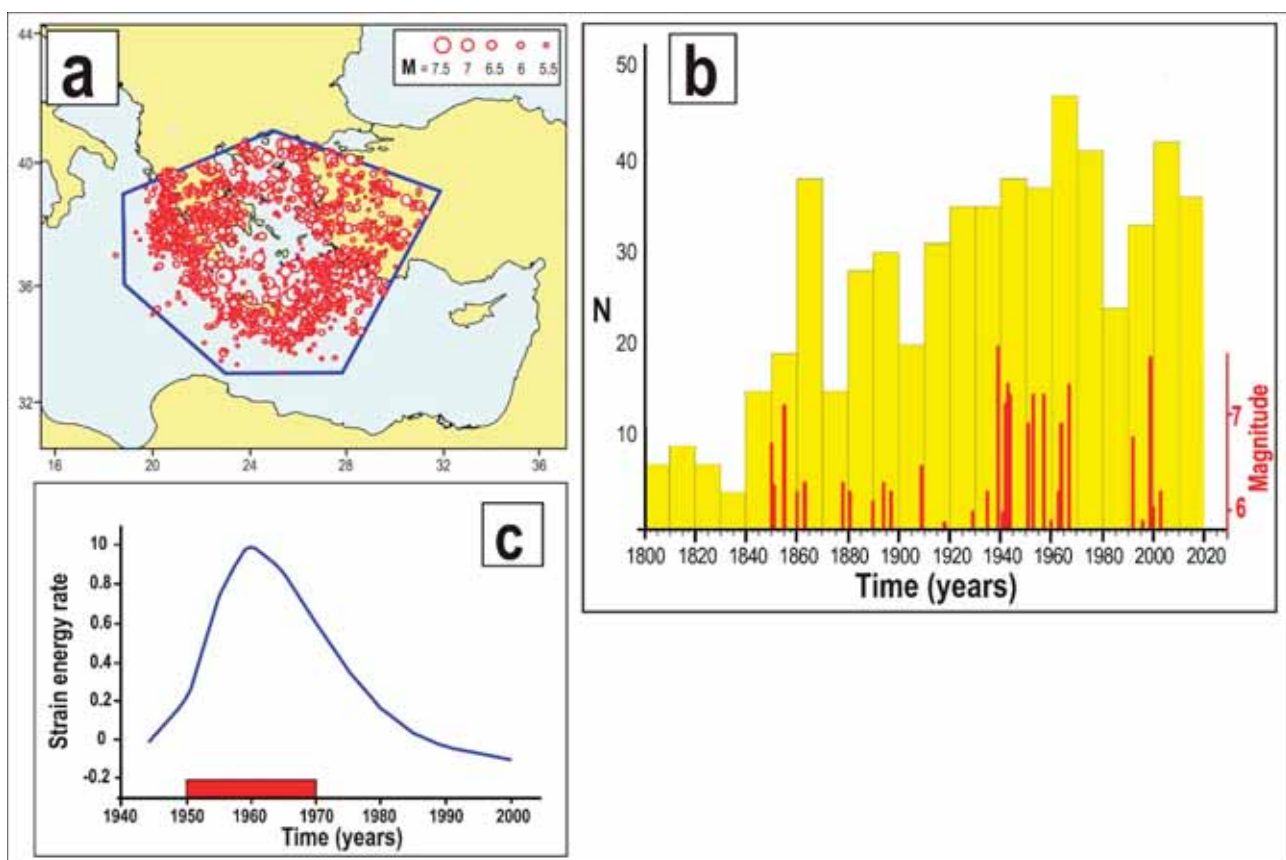

Figure 6. (**a**) Contours of the Aegean zone (blue line) that can be tectonically connected with the westward motion of Anatolia. (**b**) Time pattern (yellow bars) of the number of major earthquakes with M > 5.5 in the Aegean area during the 1800–2024 time interval. The red segments over the yellow bars indicate the time pattern of major earthquakes along the NAF (as in Figure 4). (**c**) Time pattern of the strain energy release rate in the central Aegean zone, triggered by a displacement of 7 m at the eastern Anatolia zone in 1939 (taken from [11]). The time interval during which the strain energy rate overcomes 70% of its maximum value is evidenced by the red bar along the time axis. Seismicity data as in Figures 4 and 5.

Another significant aspect of the NAF seismic sequence is that fault activations propagated westward over time. This trend indicates that the previous strain accumulation mainly developed in the eastern Anatolian zone, as implied by the geodynamic interpretation proposed here. Conversely, the slab-pull mechanism implies that strain accumulation

would mainly develop in the southern Aegean zone in response to the SW-ward retreat of the Hellenic arc [164].

A further piece of evidence that may provide insights into the tectonic context of the study area is the fact that subcrustal seismicity in the Aegean zone (Figure 7) has undergone a considerable slowdown since 1940. Considering that this time interval mainly corresponds to when the most intense perturbation of the velocity field induced by post-1939 seismic sequence reached the southern Aegean zone, one could suppose that the expected progressive SW-ward displacement of the Aegean zone had increased friction at the Hellenic trench faults, slowing down subduction and then mitigating the related seismicity.
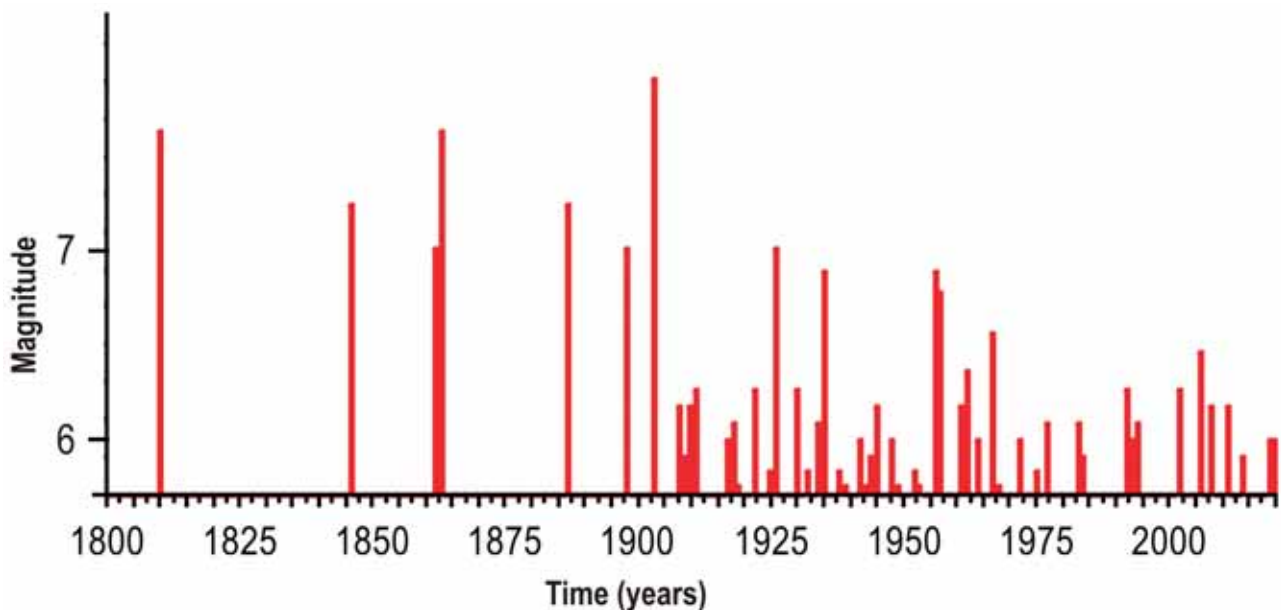

Figure 7. Time pattern of sub-crustal earthquakes (depth greater than 50 km) under the Aegean zone. Seismicity data as in Figure 5.

5. Possible Connections Between the Seismic Activations of the Main Faults Bordering the Arabian and Eastern Anatolian Structures

Driven by the spreading of the Red Sea and the Aden gulf, the Arabian plate tries to move roughly northward. This motion is accommodated by shortening processes at the collision zone with Eurasia. At the northeastern front (Zagros), the shortening is accommodated by underthrusting, uplift and lateral escape of masses in a relatively wide zone (e.g., [164,165]). At the northwestern front, the shortening is accommodated by uplift and the westward escape of the Anatolian wedge. The decoupling of Arabia from Nubia is mainly allowed by strong earthquakes along the Dead Sea Fault (DSF). The activities in the above seismic zones are connected to each other, as the decoupling earthquakes in one fault zone may increase stress at the other, still blocked, faults. To tentatively evaluate the reliability of this hypothesis, we have considered the distribution of major earthquakes that have occurred since 1600 in the northern Arabian and eastern Anatolian (EAF and NAF) zones (Figure 8). To evidence the main seismic phases at the above fault systems, we have considered four time intervals (Figure 8c–f).

In the long first phase (1600–1871, Figure 8c), seismic activity mostly occurred along the DSF and the Zagros thrust front. The transcurrent slips along various sectors of DSF allowed the western side of the Arabian indenter to decouple from Nubia, while the activation of several thrust faults in the Zagros zone accommodated a northward displacement of the Arabian indenter. One may expect that these partial accelerations of the indenter increased stress at the sectors of the northern Arabian front that were still blocked. In particular, this phenomenon may have increased shear stress at the EAF and NAF. This hypothesis may explain what happened in the next phases, when four strong earthquakes (1874 M = 7.1;

1875 M = 6.7; 1893 M = 7.1; 1905 M = 6.8) occurred along the EAF (Figure 8d) and then, since 1939, a series of major shocks have activated the entire NAF: 1939 M = 7.9; 1942 M = 7.0; 1943 M = 7.6; 1944 M = 7.4; 1957 M = 7.0; 1967 M = 7.1; 1999 M = 7.4 (Figure 8e).
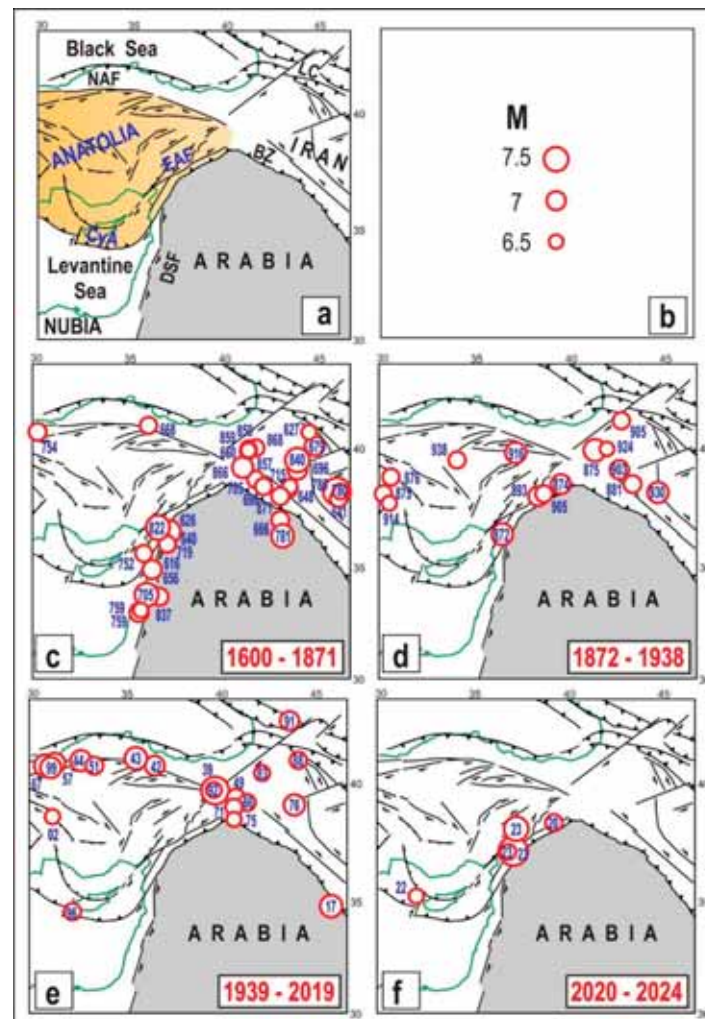

Figure 8. (**a**) Tectonic sketch of the collision zone between the Arabian indenter (grey) and the extruding Anatolian wedge (brown). BZ = Bitlis–Zagros thrust front, CyA = Cyprus Arc, DSF = Dead Sea fault system, EAF = East Anatolian fault, LC = Lesser Caucasus, NAF = North Anatolian fault. Tectonic symbols as in Figure 1. (**b**) Scale of magnitudes. (**c**–**f**) Major earthquakes (M ≥ 6.5) in the time intervals reported in the pictures. Seismicity data as in Figure 5.

It is reasonable to think that the exceptional decoupling that accompanied the seismic sequence along the NAF allowed a marked westward displacement of the Anatolian wedge, causing a strong increase in shear stress at the EAF. This hypothesis could explain why three strong earthquakes recently occurred at that fault (2020 M = 6.8, 2023 M = 7.8, 7.7, Figure 8f). It can finally be noted that these last shocks only occurred at sectors of the EAF that were not activated by the major 1874–1905 seismic crisis [166].

6. Conclusions

The complex Neogene tectonic evolution of the Anatolian–Aegean–Balkan system is explained as an effect of the westward migration and deformation that the Tethyan belt has undergone in response to the indentation of the Arabian indenter. The fact that the inner core of the belt has undergone strong bending without significant interruptions suggests a mainly ductile rheological behavior of that structure. Conversely, the two orogenic belts

that flanked the inner core underwent major fragmentations (in the zones of maximum bending), indicating a mainly brittle character. Most of the tectonic processes took place since the late Miocene, after the collision of the Tethyan belt with the Adriatic domain, which accelerated the bending of that system. The most evident examples of ductile versus brittle tectonics are given by the formation of the Cyprus and Aegean arcs, where the inner cores underwent a marked bending with no fragmentation, whereas the outer orogenic belts were affected by major breaks in the zones of strongest curvature. The proposed interpretation may provide plausible explanations for the evolution of the Peloponnesus and Creta–Rhodes belt sectors, the formation of the Cretan and Cilicia–Adana basins and the complex set of tectonic processes in the northern Aegean and Balkan regions.

In particular, the tectonic setting in the Serbo–Macedonian massif (mainly the Struma zone) is explained as an effect of two simultaneous driving mechanisms. The roughly NW-ward motion and clockwise rotation of the Rhodope massif (stressed by northwestern Anatolia), induces a compressional regime in the Serbo–Macedonian zone, while the westward motion of the Aegean Tethyan belt (Epirus) induces extension in the same zone. In the long term, the combined effect of these two mechanisms produced a S–N extension in the SMM zone, as indicated by geological data. In the short term, the SMM zone can be affected by compressional or tensional deformations, depending on the previous seismic activity in the NAF or the Epirus thrust front, respectively. After intense seismic crises in the NAF, the consequent westward displacement of Anatolia stresses the Rhodope massif, inducing a compressional regime in the SMM zone. This effect propagates with velocities controlled by the rheological nature of the structures involved. The results of numerical modellings suggest that such perturbation can affect the Balkan zones for several decades. This hypothesis can explain why, during the activation of the NAF since the 1939, seismic activity in the SMM zone was rather low (Figure 4). The above view can also help to understand why a compressional strain field is now recognized, by geodetic data, in the Struma and Krupnic fault zones, where geological evidence indicates an extensional regime. When instead, strong shocks occur in the Epirus thrust front, the consequent westward displacement of the western Aegean Tethyan belt temporarily (decades) induces an extensional regime in the SMM zone. This can explain why the most intense seismic crises in the SMM zone occurred after or during the most intense seismic periods in the Epirus (Figure 4).

The time pattern of the annual number of major earthquakes (M > 5.5) in the Aegean zone during the last two centuries (1800–2024, Figure 6) shows the highest values in the time interval 1950–1980, when that zone was undergoing the highest effects of the post-seismic relaxation triggered by the strong NAF seismic sequence since 1939. This time correspondence may support the hypothesis that tectonic activity in the Aegean zone is mainly influenced by the westward displacement of Anatolia.

The distribution of major earthquakes since 1600 (Figure 8) in the Arabian and eastern Anatolian zones may provide insights into how the activations of the main fault systems are connected to each other. In particular, this evidence indicates that seismic activity mainly occurred along the northern Arabian front and the Dead Sea fault system for a long time interval, during which no major earthquakes occurred at the EAF and NAF. This evidence may suggest that at present, after the last strong seismic crises in the NAF (1939–1999) and EAF (1874–1905 and 2023), the probability of major seismic crises along these fault systems may be significantly low for a long time interval. However, one must be aware that evaluating the statistical significance of seismicity patterns inferred from relatively short seismic histories (in zones characterized by long recurrence times) may be very difficult. Furthermore, we can hardly understand if the strain accumulated in the Anatolian wedge has been completely released by the last seismic crises at the NAF and EAF faults. Thus, it seems opportune to monitor the ongoing strain rate in the most dangerous seismic zones through geodetic and geophysical observations.

References

1. Royden, L.H. Evolution of retreating subduction boundaries formed during continental collision. *Tectonics* **1993**, *12*, 629–638. [CrossRef]
2. Carminati, E.; Doglioni, C. Mediterranean tectonics. *Encycl. Geol.* **2005**, *2*, 135–146.
3. Burchfiel, B.; Nakov, R.; Dumurdzanov, N.; Papanikolaou, D.; Tzankov, T.; Serafimovski, T.; King, R.; Kotzev, V.; Todosov, A.; Nurce, B. Evolution and dynamics of the Cenozoic tectonics of the South Balkan extensional system. *Geosphere* **2008**, *4*, 919–938. [CrossRef]
4. Faccenna, C.; Becker, T.W.; Auer, L.; Billi, A.; Boschi, L.; Brun, J.P.; Capitanio, F.A.; Funiciello, F.; Horvàth, F.; Jolivet, L.; et al. Mantle dynamics in the Mediterranean. *Rev. Geophys.* **2014**, *52*, 283–332. [CrossRef]
5. Menant, A.; Sternai, P.; Jolivet, L.; Guillou-Frottier, L.; Gerya, T. 3D numerical modeling of mantle flow, crustal dynamics and magma genesis associated with slab roll-back and tearing: The eastern Mediterranean case. *Earth Planet. Sci. Lett.* **2016**, *442*, 93–107. [CrossRef]
6. Menant, A.; Jolivet, L.; Vrielynck, B. Kinematic reconstructions and magmatic evolution illuminating crustal and mantle dynamics of the eastern Mediterranean region since the late Cretaceous. *Tectonophysics* **2016**, *675*, 103–140. [CrossRef]
7. Brun, J.P.; Faccenna, C.; Gueydan, F.; Sokoutis, D.; Philippon, M.; Kydonakis, K.; Gorini, C. The two-stage Aegean extension, from localized to distributed, a result of slab rollback acceleration. *Can. J. Earth Sci.* **2016**, *53*, 1142–1157. [CrossRef]
8. Reilinger, R.; McClusky, S.; Vernant, P.; Lawrence, S.; Ergintav, S.; Cakmak, R.; Ozener, H.; Kadirov, F.; Guliev, I.; Stepanyan, R.; et al. GPS constraints on continental deformation in the Africa-Arabia-Eurasia continental collision zone and implications for the dynamics of plate interactions. *J. Geophys. Res.* **2006**, *111*, B05411. [CrossRef]
9. Nocquet, J.-M. Present-day kinematics of the Mediterranean: A comprehensive overview of GPS results. *Tectonophysics* **2012**, *579*, 220–242. [CrossRef]
10. Mantovani, E.; Viti, M.; Cenni, N.; Albarello, D.; Babbucci, D. Short and long-term deformation patterns in the Aegean-Anatolian systems: Insights from space geodetic data (GPS). *Geophys. Res. Lett.* **2001**, *28*, 2325–2328. [CrossRef]
11. Cenni, N.; D'onza, F.; Viti, M.; Mantovani, E.; Albarello, D.; Babbucci, D. Post seismic relaxation processes in the Aegean-Anatolian system: Insights from space geodetic data (GPS) and geological/geophysical evidence. *Boll. Geofis. Teor. Appl.* **2002**, *43*, 23–36.
12. Tapponnier, P. Evolution tectonique du systèmealpinenMéditerranée: Poinçonnement et écrasementrigide-plastique. *Bull. Soc. Géol. Fr.* **1977**, *19*, 437–460. [CrossRef]
13. Sengör, A.M.Ç.; Görür, N.; Saroglu, F. Strike slip faulting and related basin formation in zones of tectonic escape: Turkey as a case study. In *Strike Slip Deformation, Basin Formation, and Sedimentation*; Biddle, K.T., Christie-Blick, N., Eds.; Society of Economic Paleontologists and Mineralogists: Tulsa, OK, USA, 1985; Volume 37, pp. 227–264.
14. Taymaz, T.; Jackson, J.; McKenzie, D. Active tectonics of the north and central Aegean Sea. *Geophys. J. Int.* **1991**, *106*, 433–490. [CrossRef]
15. Armijo, R.; Meyer, B.; Hubert, A.; Barka, A. Westward propagation of the North Anatolian fault into the northern Aegean: Timing and kinematics. *Geology* **1999**, *27*, 267–270. [CrossRef]
16. Armijo, R.; Flerit, F.; King, G.; Meyer, B. Linear elastic fracture mechanics explains the past and present evolution of the Aegean. *Earth Planet. Sci. Lett.* **2003**, *217*, 85–95. [CrossRef]
17. Mantovani, E.; Viti, M.; Babbucci, D.; Tamburelli, C.; Albarello, D. Geodynamic correlation between the indentation of Arabia and the Neogene tectonics of the central-eastern Mediterranean region. In *Postcollisional Tectonics and Magmatism in the Mediterranean Region and Asia*; Geological Society of America Special Papers; Dilek, Y., Pavlides, S., Eds.; Geological Society of America: Boulder, CO, USA, 2006; Volume 409, pp. 15–41.
18. Mantovani, E.; Babbucci, D.; Tamburelli, C.; Viti, M. Late Cenozoic evolution and present tectonic setting of the Aegean–Hellenic Arc. *Geosciences* **2022**, *12*, 104. [CrossRef]
19. Mantovani, E.; Viti, M.; Babbucci, D.; Tamburelli, C.; Hoxha, I.; Piccardi, L. Geodynamics of the South Balkan and Northern Aegean Regions Driven by the Westward Escape of Anatolia. *Int. J. Geosci.* **2023**, *14*, 480–504. [CrossRef]
20. Mantovani, E.; Viti, M.; Babbucci, D.; Tamburelli, C. *Neogenic Evolution of the Mediterranean Region: Geodynamics, Tectonics and Seismicity*; Springer Nature: Cham, Switzerland, 2024; p. 174, ISBN 3031621492.
21. Viti, M.; Mantovani, E.; Babbucci, D.; Tamburelli, C.; Caggiati, M.; Riva, A. Basic role of extrusion processes in the Late Cenozoice of the western and central Mediterranean belts. *Geosciences* **2021**, *11*, 499. [CrossRef]

22. Mantovani, E.; Viti, M.; Babbucci, D.; Tamburelli, C.; Cenni, N. Geodynamics of the central-western Mediterranean region: Plausible and non-plausible driving forces. *Mar. Pet. Geol.* **2020**, *113*, 104121. [CrossRef]

23. Viti, M.; Mantovani, E.; Babbucci, D.; Tamburelli, C. Plate kinematics and geodynamics in the Central Mediterranean. *J. Geodyn.* **2011**, *51*, 190–204. [CrossRef]

24. Robertson, A.H.F.; Dixon, J.E.; Brown, S.; Collins, A.; Morris, A.; Pickett, E.A.; Sharp, I.; Ustaömer, T. Alternative tectonic models for the Late Palaeozoic-Early Tertiary development of Tethys in the Eastern Mediterranean region. In *Paleomagnetism and Tectonics of the Mediterranean Region*; Morris, A., Tarlino, D.H., Eds.; Geological Society of London, Special Publication: London, UK, 1996; Volume 105, pp. 239–263.

25. Dercourt, J.; Zonenshain, L.P.; Ricou, L.E.; Kazmin, V.G.; Le Pichon, X.; Knipper, A.L.; Grandjacquet, C.; Sbortshikov, I.M.; Geyssant, J.; Lepvrirer, C.; et al. Geological Evolution of the Tethys Belt from the Atlantic to the Pamirs since the LIAS. *Tectonophysics* **1986**, *123*, 241–315. [CrossRef]

26. Ring, U.; Layer, P.W. High-pressure metamorphism in the Aegean, eastern Mediterranean: Underplating and exhumation from the Late Cretaceous until the Miocene to Recent above the retreating Hellenic subduction zone. *Tectonics* **2003**, *22*, 1–23. [CrossRef]

27. Golonka, J. Plate tectonic evolution of the southern margin of Eurasia in the Mesozoic and Cenozoic. *Tectonophysics* **2004**, *381*, 235–273. [CrossRef]

28. Dilek, Y.; Furnes, H. Tethyan ophiolites and Tethyan seaways. *J. Geol. Soc. Lond.* **2019**, *176*, 899–912. [CrossRef]

29. Dilek, Y.; Thy, P.; Hacker, B.; Grundvig, S. Structure and petrology of Tauride ophiolites and mafic dike intrusions (Turkey): Implications for the Neotethyan ocean. *Geol. Soc. Am. Bull.* **1999**, *111*, 1192–1216. [CrossRef]

30. Robertson, A.H.F. Overview of the genesis and emplacement of Mesozoic ophiolites in the Eastern Mediterranean Tethyan region. *Lithos* **2002**, *65*, 1–67. [CrossRef]

31. Van Hinsbergen, D.J.J.; Maffione, M.; Plunder, A.; Kaymakcı, N.; Ganerød, M.; Hendriks, B.W.H.; Corfu, F.; Gürer, D.; de Gelder, G.I.N.O.; Peters, K.; et al. Tectonic evolution and paleogeography of the Kırşehir Block and the Central Anatolian Ophiolites, Turkey. *Tectonics* **2016**, *35*, 983–1014. [CrossRef]

32. McPhee, P.J.; Altıner, D.; van Hinsbergen, D.J.J. First balanced cross section across the Taurides fold-thrust belt: Geological constraints on the subduction history of the Antalya slab in southern Anatolia. *Tectonics* **2018**, *37*, 3738–3759. [CrossRef] [PubMed]

33. Ricou, L.E.; Burg, J.P.; Godfriaux, I.; Ivanov, Z. Rhodope and Vardar: The metamorphic and the olistostromic paired belts related to the Cretaceous subduction under Europe. *Geodin. Acta* **1998**, *11*, 285–309. [CrossRef]

34. Okay, A.I.; Tüysüz, O. Tethyan sutures of northern Turkey. In *The Mediterranean Basins: Tertiary Extension within the Alpine Orogen*; Durand, B., Jolivet, L., Horvath, F., Seranne, M., Eds.; Geological Society of London, Special Publications: London, UK, 1999; Volume 156, pp. 475–515.

35. Gessner, K.; Ring, U.; Passchier, C.W.; Güngör, T. How to resist subduction: Evidence for large-scale out-of-sequence thrusting during Eocene collision in western Turkey. *J. Geol. Soc. Lond.* **2001**, *158*, 769–784. [CrossRef]

36. Whitney, D.L.; Teyssier, C.; Dilek, Y.; Fayon, A.K. Metamorphism of the Central Anatolian Crystalline Complex, Turkey: Influence of orogen normal collision vs. wrench-dominated tectonics on P-T-t paths. *J. Metamorph. Geol.* **2001**, *19*, 411–432. [CrossRef]

37. Dilek, Y.; Sandvol, E. Seismic structure, crustal architecture and tectonic evolution of the Anatolian-African Plate Boundary and the Cenozoic Orogenic Belts in the Eastern Mediterranean Region. In *Ancient Orogens and Modern Analogues*; Murphy, J.B., Keppie, J.D., Hynes, A.J., Eds.; Geological Society of London, Special Publications: London, UK, 2009; Volume 327, pp. 127–160. [CrossRef]

38. Jolivet, L.; Augier, R.; Faccenna, C.; Negro, F.; Rimmele, G.; Agard, P.; Robin, C.; Rossetti, F.; Crespo-Blanc, A. Subduction, convergence and the mode of backarc extension in the Mediterranean region. *Bull. Société Géologique Fr.* **2008**, *179*, 525–550. [CrossRef]

39. Laurent, V.; Jolivet, L.; Roche, V.; Augier, R.; Scaillet, S.; Cardello, G.L. Strain localization in a fossilized subduction channel: Insights from the Cycladic Blueschist Unit (Syros, Greece). *Tectonophysics* **2016**, *672*, 150–169. [CrossRef]

40. Roche, V.; Bouchot, V.; Beccaletto, L.; Jolivet, L.; Guillou-Frottier, L.; Tuduri, J.; Bozkurt, E.; Oguz, K.; Tokay, B. Structural, lithological, and geodynamic controls on geothermal activity in the Menderes geothermal Province (Western Anatolia, Turkey). *Int. J. Earth Sci.* **2019**, *108*, 301–328. [CrossRef]

41. Royden, L.H.; Burchfiel, B.C. Are systematic variations in thrust belt style related to plate boundary processes? (the western Alps versus the Carpathians). *Tectonics* **1989**, *8*, 51–61. [CrossRef]

42. Schmid, S.M.; Fügenschuh, B.; Kounov, A.; Matenco, L.; Nievergelt, P.; Oberhansli, R.; Pleuger, J.; Schefer, S.; Schuster, R.; Tomljenovic, B.; et al. Tectonic units of the Alpine collision zone between Eastern Alps and western Turkey. *Gondwana Res.* **2020**, *78*, 308–374. [CrossRef]

43. Vecsey, L.; Plomerová, J.; Babuška, V.; PASSEQ Working Group. Mantle lithosphere transition from the East European Craton to the Variscan Bohemian Massif imaged by shear-wave splitting. *Solid Earth* **2014**, *5*, 779–792. [CrossRef]

44. Mantovani, E.; Viti, M.; Babbucci, D.; Albarello, D. Nubia-Eurasia kinematics: An alternative interpretation from Mediterranean and North Atlantic evidence. *Ann. Geophys.* **2007**, *50*, 311–336. [CrossRef]

45. Andrieux, J.; Över, S.; Poisson, A.; Bellier, O. The North Anatolian Fault Zone: Distributed Neogene deformation in its northward convex part. *Tectonophysics* **1995**, *243*, 135–154. [CrossRef]

46. Sakınç, M.; Yaltirak, C.; Oktay, F.Y. Palaeogeographical evolution of the Thrace Neogene Basin and the Tethys-Paratethys relations at northwestern Turkey (Thrace). *Palaeogeogr. Palaeoclimatol. Palaeoecol.* **1999**, *153*, 17–40. [CrossRef]

47. Zagorchev, I. Geodetic measurements, neotectonics and recent tectonics in SW Bulgaria. *Geod. Bulg. Geophys. J.* **2006**, *17*, 3–14.

48. Csontos, L.; Vörös, A. Mesozoic plate tectonic reconstruction of the Carpathian region. *Palaeogeogr. Palaeoclimatol. Palaeoecol.* **2004**, *210*, 1–56. [CrossRef]

49. Linzer, H.G.; Frisch, W.; Zweigel, P.; Girbacea, R.; Hann, H.P.; Moser, F. Kinematic evolution of the Romanian Carpathians. *Tectonophysics* **1998**, *297*, 133–156. [CrossRef]

50. Oszczypko, N. Late Jurassic-Miocene evolution of the Outer Carpathian fold-and-thrust belt and its foredeep basin (Western Carpathians, Poland). *Geol. Quart.* **2006**, *50*, 169–194.

51. Horváth, F.; Musitza, B.; Balázsb, A.; Véghd, A.; Uhrine, A.; Nádorc, A.; Koroknaia, B.; Papd, N.; Tótha, T.; Wóruma, G. Evolution of the Pannonian Basin and its geothermal resources. *Geothermics* **2015**, *53*, 328–352. [CrossRef]

52. Gallais, F.; Gutscher, M.A.; Graindorge, D.; Chamot-Rooke, N.; Klaeschen, D.A. Miocene tectonic inversion in the Ionian Sea (Central Mediterranean): Evidence from multichannel seismic data. *J. Geophys. Res.* **2011**, *116*, B12108. [CrossRef]

53. Doutsos, T.; Kontopoulos, N.; Frydas, D. Neotectonic evolution of northwestern-continental Greece. *Geol. Rundsch.* **1987**, *76*, 433–450. [CrossRef]

54. Mercier, J.; Sorel, D.; Simeakis, K. Changes in the state of stress in the overriding plate of a subduction zone: The Aegean Arc from the Pliocene to the Present. *Ann. Tectonicae* **1987**, *1*, 20–39.

55. Viti, M.; Albarello, D.; Mantovani, E. Rheological profiles in the Central-Eastern Mediterranean. *Annnals Geophys.* **1997**, *40*, 849–864.

56. Moulas, E.; Schenker, F.L.; Burg, J.P.; Kostopoulos, D. Metamorphic conditions and structural evolution of the Kesebir-Kardamos dome: Rhodope metamorphic complex (Greece-Bulgaria). *Int. J. Earth Sci.* **2017**, *106*, 2667–2685. [CrossRef]

57. Mercier, J.L.; Simeakis, K.; Sorel, D.; Vergely, P. Extensional tectonic regimes in the Aegean basins during the Cenozoic. *Basin Res.* **1989**, *2*, 49–71. [CrossRef]

58. Mascle, J.; Martin, L. Shallow structure and recent evolution of the Aegean Sea: A synthesis based on continuous reflection profiles. *Mar. Geol.* **1990**, *94*, 271–299. [CrossRef]

59. Meulenkamp, J.E.; Van Der Zwan, G.J.; Van Wamel, W.A. On late Miocene to recent vertical motions in the Cretan segment of the Hellenic arc. *Tectonophysics* **1994**, *234*, 53–72. [CrossRef]

60. Kokkalas, S.; Xypolias, P.; Koukouvelas, I.; Doutsos, T. Postcollisional contractional and extensional deformation in the Aegean Region. In *Post Collisional Tectonics and Magmatism in the Mediterranean Region and Asia*; Dilek, Y., Pavlides, S., Eds.; Geological Society of America: Boulder, NV, USA, 2006; Volume 409, pp. 97–123. [CrossRef]

61. Jolivet, L.; Labrousse, L.; Agard, P.; Lacombe, O.; Bailly, V.; Lecomte, E.; Mouthereau, F.; Mehl, C. Rifting and shallow-dipping detachments, clues from the Corinth Rift and the Aegean. *Tectonophysics* **2010**, *483*, 287–304. [CrossRef]

62. Armijo, R.; Meyer, B.; King, G.C.P.; Rigo, A.; Papanastassiou, D. Quaternary evolution of the Corinth rift and its implications for the late Cenozoic evolution of the Aegean. *Geophys. J. Int.* **1996**, *126*, 11–53. [CrossRef]

63. Pérouse, E.; Sébrier, M.; Braucher, R.; Chamot-Rooke, N.; Bourlès, D.; Briole, P.; Sorel, D.; Dimitrov, D.; Arsenikos, S. Transition from collision to subduction in Western Greece: The Katouna-Stamna active fault system and regional kinematics. *Int. J. Earth Sci.* **2016**, *106*, 967–989. [CrossRef]

64. Kempler, D.; Ben Avraham, Z. The tectonic evolution of the Cyprean Arc. *Ann. Tectonicae* **1987**, *1*, 58–71.

65. Kempler, D.; Garfunkel, Z. Structures and kinematics in the northeastern Mediterranean: A study of an irregular plate boundary. *Tectonophysics* **1994**, *234*, 19–32. [CrossRef]

66. Robertson, A.H.F. Mesozoic-Tertiary tectonic-sedimentary evolution of a south Tethyan oceanic basin and its margins in southern Turkey. In *Tectonics and Magmatism in Turkey and the Surrounding Area*; Bozkurt, E., Winchester, J.A., Piper, J.D.A., Eds.; Geological Society of London, Special Publications: London, UK, 2000; Volume 173, pp. 97–138.

67. Günes, P.; Aksu, A.; Hall, J. Structural framework and deformation history of the western Cyprus Arc. *Tectonophysics* **2018**, *744*, 438–457. [CrossRef]

68. Aksu, A.E.; Calon, T.J.; Hall, J.; Mansbridge, S.; Yaşar, D. The Cilicia–Adana basin complex, Eastern Mediterranean: Neogene evolution of an active fore-arc basin in an obliquely convergent margin. *Mar. Geol.* **2005**, *221*, 121–159. [CrossRef]

69. Işler, F.I.; Aksu, A.E.; Hall, J.; Calon, T.J.; Yaşar, D. Neogene development of the Antalya Basin, Eastern Mediterranean: An active fore-arc basin adjacent to an arc junction. *Mar. Geol.* **2005**, *221*, 237–265. [CrossRef]

70. Avigad, D.; Ziv, A.; Garfunkel, Z. Ductile and brittle shortening, extension-parallel folds and maintenance of crustal thickness in the central Aegean (Cyclades, Greece). *Tectonics* **2001**, *20*, 277–287. [CrossRef]

71. Virgo, S.; von Hagke, C.; Urai, J.L. Multiphase boudinage: A case study of amphibolites in marble in the Naxos migmatite core. *Solid Earth* **2018**, *9*, 91–113. [CrossRef]

72. Searle, M.P.; Lamont, T.N. Compressional origin of the Aegean Orogeny, Greece. *Geosci. Front.* **2022**, *13*, 101049. [CrossRef]

73. Yılmaz, Y.; Genç, S.C.; Gürer, F.; Bozcu, M.; Yılmaz, K.; Karacik, Z.; Altunkaynak, S.; Elmas, A. When did the western Anatolian grabens begin to develop? In *Tectonics and Magmatism in Turkey and the Surrounding Area*; Bozkurt, E., Winchester, J.A., Piper, J.D.A., Eds.; Geological Society of London, Special Publications: London, UK, 2000; Volume 173, p. 353.

74. Kokkalas, S.; Aydin, A. Is there a link between faulting and magmatism in the south-central Aegean Sea? *Geol. Mag.* **2013**, *150*, 193–224. [CrossRef]

75. Le Pichon, X.; Sengör, A.M.C.; Kende, J.; I'mren, C.; Henry, P.; Grall, C.; Karabulut, H. Propagation of a strike-slip plate boundary within an extensional environment: The westward propagation of the North Anatolian Fault. *Can. J. Earth Sci.* **2016**, *53*, 1416–1439. [CrossRef]

76. Lazos, I.; Sboras, S.; Pikridas, C.; Pavlides, S.; Chatzipetros, A. Geodetic analysis of the tectonic crustal deformation pattern in the North Aegean Sea, Greece. *Mediterr. Geosci. Rev.* **2021**, *3*, 79–94. [CrossRef]

77. Papazachos, B.C.; Dimitriadis, S.T.; Panagiotopoulos, D.G.; Papazachos, C.B.; Papadimitriou, E.E. Deep structure and active tectonics of the southern Aegean volcanic arc. The South Aegean Active Volcanic Arc: Present Knowledge and Future Perspectives. *Dev. Volcanol.* **2005**, *7*, 47–64. [CrossRef]

78. Pe-Piper, G.; Piper, D.J.W. The South Aegean active volcanic arc: Relationships between magmatism and tectonics. *Dev. Volcanol.* **2005**, *7*, 113–133. [CrossRef]

79. Schaarschmidt, A.; Haase, K.M.; Voudouris, P.C.; Melfos, V.; Klemd, R. Migration of arc magmatism above mantle wedge diapirs with variable sediment contribution in the Aegean. *Geochem. Geophys. Geosystems* **2021**, *22*, e2020GC009565. [CrossRef]

80. Fytikas, M.; Innocenti, F.; Manetti, P.; Mazzuoli, R.; Peccerillo, A.; Villari, L. Tertiary to Quaternary evolution of volcanism in the Aegean region. In *The Geological Evolution of the Eastern Mediterranean*; Dixon, J.E., Robertson, A.H.F., Eds.; Geological Society of London: London, UK, 1984; Volume 17, pp. 687–699.

81. Kassaras, I.; Kapetanidis, V.; Ganas, A.; Tzanis, A.; Kosma, C.; Karakonstantis, A.; Valkaniotis, S.; Chailas, S.; Kouskouna, V.; Papadimitriou, P. The New Seismotectonic Atlas of Greece (v1.0) and Its Implementation. *Geosciences* **2020**, *10*, 447. [CrossRef]

82. Milia, A.; Torrente, M.M. Late-Quaternary volcanism and transtensional tectonics in the Bay of Naples, Campanian continental margin, Italy. *Mineral. Petrol.* **2003**, *79*, 49–65. [CrossRef]

83. Acocella, V.; Funiciello, R. Transverse Systems along the Extensional Tyrrhenian Margin of Central Italy and Their Influence on Volcanism. *Tectonics* **2006**, *25*, TC2003. [CrossRef]

84. Riller, U.; Petrinovic, I.; Ramelow, J.; Strecker, M.; Oncken, O. Late Cenozoic Tectonism, Collapse Caldera and Plateau Formation in the Central Andes. *Earth Planet. Sci. Lett.* **2001**, *188*, 299–311. [CrossRef]

85. Khodayar, M.; Einarsson, P. Strike-slip faulting, normal faulting, and lateral dike injections along a single fault: Field example of the Gljúfurá fault near a Tertiary oblique rift-transform zone, Borgarfjörður, west Iceland. *J. Geophys. Res. Solid Earth* **2002**, *107*, ETG-5. [CrossRef]

86. Mann, P. Global catalogue, classification and tectonic origins of restraining-and releasing bends on active and ancient strike-slip fault systems. *Geol. Soc. Lond. Spec. Publ.* **2007**, *290*, 13–142. [CrossRef]

87. Tibaldi, A.; Pasquare, F.; Tormey, D. Volcanism in Reverse and Strike-Slip Fault Settings. In *New Frontiers in Integrated Solid Earth Sciences, International Year of Planet Earth*; Cloetingh, S., Negendank, J., Eds.; Springer: Dordrecht, The Netherlands, 2010; pp. 318–348. [CrossRef]

88. Feuillet, N.; Beauducel, F.; Tapponnier, P. Tectonic context of moderate to large historical earthquakes in the Lesser Antilles and mechanical coupling with volcanoes. *J. Geophys. Res.* **2011**, *116*, B10308. [CrossRef]

89. Spacapan, J.B.; Galland, O.; Planke, S.; Leanza, H.A. Control of strike-slip fault on dyke emplacement and morphology. *J. Geol. Soc.* **2016**, *173*, 573–576. [CrossRef]

90. Elkhedr, I.; Abd El-Motaal, E.; Lashin, A.; Alfaifi, H.J.; Qaysi, S.; Kahal, A. Faulting intersections and magma-feeding zones in Tihamat-asir, Southeast red sea rift: Aeromagnetic and structural perspective. *J. Afr. Earth Sci.* **2021**, *173*, 104044. [CrossRef]

91. Duermeijer, C.; Nyst, M.; Meijer, P.; Langereis, C.; Spakman, W. Neogene evolution of the Aegean arc: Paleomagnetic and geodetic evidence for a rapid and young rotation phase. *Earth Planet. Sci. Lett.* **2000**, *176*, 509–525. [CrossRef]

92. Aliaj, S. Seismotectonics of Vlora–Elbasani-Dibra Transversal Fault Zone (Albania): A Review. *Earth Sci.* **2021**, *10*, 346–357. [CrossRef]

93. Handy, M.R.; Giese, J.; Schmid, S.M.; Pleuger, J.; Spakman, W.; Onuzi, K.; Ustaszewski, K. Coupled Crust- Mantle Response to Slab Tearing, Bending and Rollback along the Dinaride-Hellenide Orogen. *Tectonics* **2019**, *38*, 2803–2828. [CrossRef]

94. Mercier, J.L. Extensional-compressional tectonics associated with the Aegean Arc: Comparison with the Andean Cordillera of south Peru-north Bolivia. *Philos. Trans. R. Soc. Lond.* **1981**, *300*, 337–355.

95. Caputo, R.; Pavlides, S. Late Cainozoic geodynamic evolution of Thessaly and surroundings (central-northern Greece). *Tectonophysics* **1993**, *223*, 339–362. [CrossRef]

96. McClusky, S.; Balassanian, S.; Barka, A.; Demir, C.; Ergintav, S.; Georgiev, I.; Gurkan, O.; Hamburger, M.; Hurst, K.; Kahle, H.; et al. Global Positioning System constraints on the plate kinematics and dynamics in the eastern Mediterranean and Caucasus. *J. Geophys. Res.* **2000**, *105*, 5695–5719. [CrossRef]

97. Kotzev, V.; Nakov, R.; Burchfiel, B.C.; King, R.; Reilinger, R. GPS study of active tectonics in Bulgaria: Results from 1996 to 1998. *J. Geodyn.* **2001**, *31*, 189–200. [CrossRef]

98. Kotzev, V.; Nakov, R.; Georgiev, T.Z.; Burchfiel, B.C.; King, R.W. Crustal motion and strain accumulation in western Bulgaria. *Tectonophysics* **2006**, *413*, 127–145. [CrossRef]

99. Van Hinsbergen, D.; Schmid, S.M. Map view restoration of Aegean-West Anatolian accretion and extension since the Eocene. *Tectonics* **2012**, *31*, 5. [CrossRef]

100. Yaltırak, C.; Alpar, B.; Yuce, H. Tectonic Elements Controlling the Evolution of the Gulf of Saros (northeastern Aegean Sea, Turkey). *Tectonophysics* **1998**, *300*, 227–248. [CrossRef]

101. Piccardi, L.; Dobrev, N.; Moratti, G.; Corti, G.; Tondi, E.; Vannucci, G.; Matova, M.; Spina, V. Overview and New Data on the Active Tectonics of Bulgaria: Towards a Comprehensive Seismotectonic Map. *Acta Volcanol.* **2013**, *25*, 67–82.
102. Dobrev, N. 3D Monitoring of Active Fault Structures In The Krupnik-Kresna Seismic Zone, SW Bulgaria. *Acta Geodyn. Geomater.* **2011**, *8*, 377–388.
103. Barka, A.A. Slip distribution along the North Atlantic fault associated with the large earthquakes of the period 1939 to 1967. *Bull. Seismol. Soc. Am* **1996**, *86*, 1238–1254. [CrossRef]
104. Karnik, V. *Seismicity of the European Area*; Part I and Part II; Springer: Dordrecht, The Netherlands, 1971.
105. Kondorskaya, N.V.; Shebalin, N.V. New catalog of strong earthquakes in the U.S.S.R. from ancient times through 1977. In *World Data Center for Solid Earth Sciences*; Solid Earth Physics: Moscow, Russia, 1982; p. 173.
106. Ambraseys, N.N.; Finkel, C.F. Seismicity of Turkey and neighbouring regions, 1899–1915. *Ann. Geophys.* **1987**, *5B*, 501–726.
107. Comninakis, P.E.; Papazachos, B.C. *A Catalogue of Earthquakes in Greece and the Surrounding Area for the Period 1901–1985*; Geophysical Laboratory Publications, University of Thessaloniki: Thessaloniki, Greece, 1986.
108. Shebalin, N.V.; Leydecker, G.; Mokrushina, N.G.; Tatevossian, R.E.; Erteleva, O.O.; Vassiliev, V.Y. *Earthquake Catalogue for Central and Southeastern Europe, 342 BC–1990 AD*; Final Report to Contract No ETNU-CT930087; European Commission: Brussels, Belgium, 1998.
109. Sbeinati, M.R.; Ryad Darawcheh, R.; Mouty, M. The historical earthquakes of Syria: An analysis of large and moderate earthquakes from 1365 B.C. to 1900 A.D. *Ann. Geophys.* **2005**, *3*, 347–435. [CrossRef]
110. Godey, S.; Bossu, R.; Guilbert, J.; Mazet-Roux, G. The Euro-Mediterranean Bulletin: A comprehensive seismological bulletin at regional scale. *Seismol. Res. Lett.* **2006**, *77*, 460–474. [CrossRef]
111. ISIDe Working Group (INGV). Italian Seismological Instrumental and Parametric Database. 2010. Available online: http://iside.rm.ingv.it (accessed on 1 June 2024).
112. Grünthal, G.; Wahlström, R. The European-Mediterranean Earthquake Catalogue (EMEC) for the last millennium. *J. Seismol.* **2012**, *16*, 535–570. [CrossRef]
113. Ekström, G.; Nettles, M.; Dziewonski, A. The global CMT project 2004–2010: Centroid-moment tensors for 13.017 earthquakes. *Phys. Earth Planet. Inter.* **2012**, *201*, 1–9. [CrossRef]
114. Makropoulos, K.; Kaviris, G.; Kouskouna, V. An updated and extended earthquake catalogue for Greece and adjacent areas since 1900. *Nat. Hazards Earth Syst. Sci.* **2012**, *12*, 1425–1430. [CrossRef]
115. Sesetyan, K.; Demircioglu, M.; Rovida, A.; Albini, P.; Stucchi, M.; Zare, M.; Viganò, D.; Locati, M. SHARE-CET, the SHARE Earthquake Catalogue for Central and Eastern Turkey Complementing the SHARE European Catalogue (SHEEC). 2013. Available online: https://www.emidius.eu/SHEEC/ (accessed on 1 June 2024).
116. Stucchi, M.; Rovida, A.; Capera, A.A.G.; Alexandre, P.; Camelbeeck, T.; Demircioglu, M.B.; Gasperini, P.; Kouskouna, V.; Musson, R.M.W.; Radulian, M.; et al. The SHARE European Earthquake Catalogue (SHEEC) 1000–1899. *J. Seismol.* **2013**, *17*, 523–544. [CrossRef]
117. Rothé, J.P. *The Seismicity of the Earth (1953–1965)*; Series of Earth Sciences; UNESCO: Brussels, Belgium, 1969; 336p.
118. Ben-Menahem, A. Earthquake catalogue for the Middle East (92 B.C.–1980 A.D). *Boll. Geofis. Teor. Appl.* **1979**, *84*, 245–310.
119. Ambraseys, N.N.; Melville, C.P. *A History of Persian Earthquakes*; Cambridge University Press: Cambridge, UK, 1982.
120. Ambraseys, N.N. Material for the investigation of the seismicity of Tripolitania (Libya). *Boll. Geof. Teor. Appl.* **1984**, *103*, 143–155.
121. Al Hakeem, K. Studying of historical earthquakes activity in Syria. In *Workshop on Historical Seismicity of Central-Eastern Mediterranean Region*; Margottini, C., Serva, L., Eds.; ENEA-IAEA: Rome, Italy, 1988.
122. Khair, K.; Karakaisis, G.F.; Papadimitriou, E.E. Seismic zonation oft he Dead Sea trasform fault area. *Ann. Geofis.* **2000**, *43*, 61–79.
123. Abde-Ramal, K.; Al-Amri, A.M.S.; Abdel-Moneit, E. Seismicity of Sinai peninsula, Egypt. *Arab J. Geosci.* **2009**, *2*, 103–118. [CrossRef]
124. Rovida, A.; Locati, M.; Camassi, R.; Lolli, B.; Gasperini, P.; Antonucci, A. *Italian Parametric Earthquake Catalogue (CPTI15), Version 3.0*; Istituto Nazionale di Geofisica e Vulcanologia (INGV): Rome, Italy, 2022. [CrossRef]
125. Jouanne, F.; Mugnier, J.L.; Koci, R.; Bushati, S.; Matev, K.; Kuka, N.; Shinko, I.; Kociu, S.; Duni, L. GPS Constraints on Current Tectonics of Albania. *Tectonophysics* **2012**, *554–557*, 50–62. [CrossRef]
126. Aliaj, S. Seismotectonics of the Albanides Collision Zone: Geometry of the Underthrusting Adria Microplate beneath the Albanides. *J. Nat. Sci. Technol.* **2020**, *51*, 1–40.
127. Ganas, A.; Elias, P.; Briole, P.; Cannavo, F.; Valkaniotis, S.; Tsironi, V.; Partheniou, E.I. Ground Deformatio and Seismic Fault Model of the M6.4 Durres (Albania) Nov. 26, 2019 Earthquake, Based on GNSS/INSAR Observations. *Geosciences* **2020**, *10*, 210. [CrossRef]
128. Vittori, E.; Blumetti, A.M.; Comerci, V.; Di Manna, P.; Piccardi, L.; Gega, D.; Hoxha, I. Geological Effects and Tectonic Environment of the November 26, 2019, Mw 6.4 Durres Earthquake (Albania). *Geophys. J. Int.* **2021**, *225*, 1174–1191. [CrossRef]
129. Del Ben, A.; Mocnik, A.; Volpi, V.; Karvelis, P. Old Domains in the South Adria Plate and Their Relationship with the West Hellenic Front. *J. Geodyn.* **2015**, *89*, 15–28. [CrossRef]
130. Hansen, S.E.; Evangelidis, C.P.; Papadopoulos, G.A. Imaging Slab Detachment within the Western Hellenic Subduction Zone. *Geochem. Geophys. Geosyst.* **2019**, *20*, 895–912. [CrossRef]

131. Valkaniotis, S.; Briole, P.; Ganas, A.; Elias, P.; Kapetanidis, V.; Tsironi, V.; Fokaefs, A.; Partheniou, H.; Paschos, P. The Mw = 5.6 Kanallaki Earthquake of 21 March 2020 in West Epirus, Greece: Reverse Fault Model from InSAR Data and Seismotectonic Implications for Apulia-Eurasia Collision. *Geosciences* **2020**, *10*, 454. [CrossRef]

132. Sachpazi, M.; Hirn, A.; Clément, C.; Haslinger, F.; Laigle, M.; Kissling, E.; Charvis, P.; Hello, Y.; Lépine, J.-C.; Sapin, M.; et al. Western Hellenic Subduction and Cephalonia Transform: Local Earthquakes and Plate Transport and Strain. *Tectonophysics* **2000**, *319*, 301–319. [CrossRef]

133. Sokos, E.; Kiratzi, A.; Gallovič, F.; Zahradník, J.; Serpetsidaki, A.; Plicka, V.; Janský, J.; Kostelecký, J.; Tselentis, G.A. Rupture Process of the 2014 Cephalonia, Greece, Earthquake Doublet (Mw6) as Inferred from Regional and Local Seismic Data. *Tectonophysics* **2015**, *656*, 131–141. [CrossRef]

134. Mavroulis, S.; Lekkas, E. Revisiting the Most Destructive Earthquake Sequence in the Recent History of Greece: Environmental Effects Induced by the 9, 11 and 12 August 1953 Ionian Sea Earthquakes. *Appl. Sci.* **2021**, *11*, 8429. [CrossRef]

135. Özbakır, A.D.; Govers, R.; Fichtner, A. The Kefalonia Transform Fault: A STEP Fault in the Making. *Tectonophysics* **2020**, *787*, 228471. [CrossRef]

136. Kokkalas, S.; Pavlides, S.; Koukouvelas, I.; Ganas, A.; Stamatopoulos, L. Paleoseismicity of the Kaparelli Fault (eastern Corinth Gulf): Evidence for Earthquake Recurrence and Fault Behaviour. *Boll. Della Soc. Geol. Ital.* **2007**, *126*, 387–395.

137. Caputo, R.; Chatzipetros, A.; Pavlides, S.; Sboras, S. The Greek Database of Seismogenic Sources (GreDaSS): State-of-the-Art for Northern Greece. *Ann. Geophys.* **2012**, *55*, 859–894. [CrossRef]

138. Papadopoulos, G.A.; Agalos, A.; Karavias, A.; Triantafyllou, I.; Parcharidis, I.; Lekkas, E. Seismic and Geodetic Imaging (DInSAR) Investigation of the March 2021 Strong Earthquake Sequence in Thessaly, Central Greece. *Geosciences* **2021**, *11*, 311. [CrossRef]

139. Koukouvelas, I.K.; Aydin, A. Fault Structure and Related Basins of the North Aegean Sea and Its Surroundings. *Tectonics* **2002**, *21*, 1–17. [CrossRef]

140. Sboras, S.; Chatzipetros, A.; Pavlides, S. North Aegean Active Fault Pattern and the 24 May 2014, Mw 6.9 Earthquake. In *Active Global Seismology: Neotectonics and Earthquake Potential of the Eastern Mediterranean Region*; Çemen, I., Yılmaz, Y., Eds.; Geophysical Monograph; Wiley: Hoboken, NJ, USA, 2017; Volume 225, pp. 239–272. [CrossRef]

141. Rangin, C.; Le Pichon, X.; Demirbag, E.; Imren, C. Strain Localization in the Sea of Marmara: Propagation of the North Anatolian Fault in a Now Inactive Pull-Apart. *Tectonics* **2004**, *23*, TC2014. [CrossRef]

142. Kiratzi, A. Source Constraints Using Ground Motion Simulations. *Bull. Geol. Soc. Greece* **2013**, *47*, 1128–1137. [CrossRef]

143. Karakaş, Ç.; Armijo, R.; Lacassin, R.; Suc, J.P.; Melinte-Dobrinescu, M.C. Crustal Strain in the Marmara Pull-Apart Region Associated with the Propagation Process of the North Anatolian Fault. *Tectonics* **2018**, *37*, 1507–1523. [CrossRef]

144. Emre, Ö.; Duman, T.Y.; Özalp, S.; Şaroğlu, F.; Olgun, Ş.; Elmacı, H.; Çan, T. Active fault database of Turkey. *Bull. Earthq. Eng.* **2018**, *16*, 3229–3275. [CrossRef]

145. Sun, Y.-S.; Melgar, D.; Ruiz-Angulo, A.; Ganas, A.; Taymaz, T.; Crowell, B.; Xu, X.; Tsironi, V.; Karasante, I.; Yolsal-Çevikbilen, S.; et al. The 2020 M_w 7.0 Samos (Eastern Aegean Sea) Earthquake: Joint source inversion of multitype data, and tsunami modelling. *Geophys. J. Int.* **2024**, *237*, 1285–1300. [CrossRef]

146. Meyer, B.; Armijo, R.; Dimitrov, D. Active faulting in SW Bulgaria: Possible surface rupture of the 1904 Struma earthquakes. *Geophys. J. Int.* **2002**, *148*, 246–255. [CrossRef]

147. Tranos, M.D. Strymon and Strymonikos Gulf Basins (Northern Greece): Implications on Their Formation and Evolution from Faulting. *J. Geodyn.* **2011**, *51*, 285–305. [CrossRef]

148. Vanneste, K.; Radulov, A.; De Martini, P.; Nikolov, G.; Petermans, T.; Verbeeck, K.; Camelbeeck, T.; Pantosti, D.; Dimitrov, D.; Shanov, S. Paleoseismologic Investigation of the Fault Rupture of the 14 April 1928 Chirpan Earthquake (M 6.8), Southern Bulgaria. *J. Geophys. Res.* **2006**, *111*, B01303. [CrossRef]

149. Barka, A.A.; Reilinger, R. Active tectonics of the eastern Mediterranean region: Deduced from GPS, neotectonic and seismicity data. *Ann. Geofis.* **1997**, *40*, 587–610. [CrossRef]

150. Nissen, E.; Cambaz, M.D.; Gaudreau, É.; Howell, A.; Karasözen, E.; Savidge, E. A reappraisal of active tectonics along the Fethiye–Burdur trend, Southwestern Turkey. *Geophys. J. Int.* **2022**, *230*, 1030–1051. [CrossRef]

151. Shaw, B.; Jackson, J. Earthquake mechanisms and active tectonics of the Hellenic subduction zone. *Geophys. J. Int.* **2010**, *181*, 966–984. [CrossRef]

152. Konstantinou, K.I.; Mouslopoulou, V.; Liang, W.-T.; Heidbach, O.; Oncken, O.; Suppe, J. Present-day crustal stress field in Greece inferred from regional-scale damped inversion of earthquake focal mechanisms. *J. Geophys. Res. Solid Earth* **2017**, *122*, 506–523. [CrossRef]

153. Hubert-Ferrari, A.; Armijo, R.; King, G.; Meyer, B.; Barka, A. Morphology, displacement, and slip rates along the North Anatolian Fault, Turkey. *J. Geophys. Res.* **2002**, *107*, 1–33. [CrossRef]

154. Barka, A.A.; Kadinsky-Cade, K. Strike-slip fault geometry in Turkey and its influence on earthquake activity. *Tectonophysics* **1988**, *7*, 663–684. [CrossRef]

155. Okay, A.I.; Tüysüz, O.; Kaya, Ş. From transpression to transtension: Changes in morphology and structure around a bend on the North Anatolian Fault in the Marmara region. *Tectonophysics* **2004**, *391*, 259–282. [CrossRef]

156. Sözbilir, H.; Sümer, Ö.; Özkaymak, Ç.; Uzel, B.; Güler, T.; Eski, S. Kinematic analysis and paleoseismology of the Edremit Fault Zone: Evidence for past earthquakes in the southern branch of the North Anatolian Fault Zone, Biga Peninsula, NW Turkey. *Geodin. Acta* **2016**, *28*, 273–294. [CrossRef]

157. Eytemiz, C.; Özel, F.E. Investigation of active tectonics of Edremit Gulf, western Anatolia (Turkey), using highresolution multi-channel marine seismic data. *Mar. Sci. Technol. Bull.* **2020**, *9*, 51–57. [CrossRef]

158. Bohnhoff, M.; Martínez-Garzón, P.; Bulut, F.; Stierle, E.; Ben-Zion, Y. Maximum Earthquake Magnitudes along Different Sections of the North Anatolian Fault Zone. *Tectonophysics* **2016**, *674*, 147–165. [CrossRef]

159. Yılmaz, H.; Over, S.; Ozden, S. Kinematics of the East Anatolian Fault Zone between Turkoglu (Kahramanmaras) and Celikhan (Adıyaman), eastern Turkey. *Earth Planets Space* **2006**, *58*, 1463–1473. [CrossRef]

160. Güvercin, S.E.; Karabulut, H.; Konca, A.Ö.; Doğan, U.; Ergintav, S. Active seismotectonics of the East Anatolian fault. *Geophys. J. Int.* **2022**, *230*, 50–69. [CrossRef]

161. Liu, C.; Lay, T.; Wang, R.; Taymaz, T.; Xie, Z.; Xiong, X.; Irmak, T.S.; Kahraman, M.; Erman, C. Complex multi-fault rupture and triggering during the 2023 earthquake doublet in southeastern Türkiye. *Nat. Commun.* **2023**, *14*, 5564. [CrossRef]

162. Anderson, D.L. Accelerated plate tectonics. *Science* **1975**, *167*, 1077–1079. [CrossRef]

163. Rydelek, P.A.; Sacks, I.S. Asthenospheric viscosity and stress diffusion: A mechanism to explain correlated earthquakes and surface deformation in NE Japan. *Geophys. J. Int* **1990**, *100*, 39–58. [CrossRef]

164. Hubert-Ferrari, A.; King, G.; Manighetti, I.; Armijo, R.; Meyer, B.; Tapponnier, P. Long-term elasticity in the continental lithosphere; modelling the Aden Ridge propagation and the Anatolian extrusion process. *Geophys. J. Int.* **2003**, *153*, 111–132. [CrossRef]

165. Stern, R.J.; Johnson, P. Continental lithosphere of the Arabian Plate: A geologic, petrologic, and geophysical synthesis. *Earth-Sci. Rev.* **2010**, *101*, 29–67. [CrossRef]

166. Karabulut, H.; Güvercin, S.E.; Hollingsworth, J.; Konca, A.Ö. Long silence on the East Anatolian Fault Zone (Southern Turkey) ends with devastating double earthquakes (6 February 2023) over a seismic gap: Implications for the seismic potential in the Eastern Mediterranean region. *J. Geol. Soc.* **2023**, *180*, jgs2023-021. [CrossRef]